Elsevier Editorial System(tm) for Journal of Hydrology or its open access mirror
Manuscript Draft

Manuscript Number: HYDROL35559R1

Title: The performance of the IMERG satellite-based product in identifying sub-daily rainfall events and their properties

Article Type: Research paper

Keywords: GPM; evaluation; Inter-event time; Depth; Intensity; Duration.

Corresponding Author: Dr. Victor Hugo Rabelo Coelho, Ph.D.

Corresponding Author's Institution: Federal University of Paraíba

First Author: Emerson S Freitas, MSc

Order of Authors: Emerson S Freitas, MSc; Victor Hugo Rabelo Coelho, Ph.D.; Yunqing Xuan, Ph.D.; Davi Melo, Ph.D.; André N Gadelha, MSc; Elias A Santos Júnior, BEng; Carlos O Galvão, Ph.D.; Geraldo Ramos, MSc; Luis Romero Barbosa, Ph.D.; George J Huffman, Ph.D.; Walt A Petersen, Ph.D.; Cristiano N Almeida, Ph.D.

Abstract: Sub-daily rainfall information is essential for many hydrological applications, but ground-based data availability is still an issue in poorly gauged regions worldwide. Satellite remote sensing missions, such as the Global Precipitation Measurement (GPM) mission, have been playing a key role in estimating sub-daily rainfall data globally. However, the quality of such information needs to be carefully evaluated. Previous studies evaluating sub-daily data from the Integrated multi-satellitE Retrievals for GPM (IMERG) product considered only the rainfall depth over pre-defined periods (e.g., hourly or half-hourly), with no analysis of the ability and quality of the product in defining the actual rainfall events and the associated properties. Thus, the objective of this study is to evaluate the performance of the IMERG Final Run Version 06B (V06B) product in capturing sub-daily rainfall events and their properties (depth, duration and intensity) over Brazil. The analysis consisted of comparing the satellite estimates against the ground-based data from 1,757 sub-daily rainfall gauges for a period of three years (2015-2017). This study used the minimum inter-event time (MIT) criterion to define independent rainfall events determined by dry periods: 1, 6 and 24 hours. Results show that IMERG can properly estimate the sub-daily rainfall depth for the three MITs considered, with the best results found in the southern part of the country. This means that the IMERG product represents a good source of sub-daily rainfall depth data for hydrological and hydroclimatic applications in Brazil. On the other hand, the evaluation shows large overestimations and underestimations of the IMERG product for rainfall duration and intensity properties, respectively. The results obtained from this study provide a reference for IMERG users who require sub-daily rainfall data based on events and further knowledge about its properties.

Suggested Reviewers: Guoqiang Tang
tgq14@mails.tsinghua.edu.cn

The performance of the IMERG satellite-based product in identifying sub-daily rainfall events and their properties

Emerson da S. Freitas[a], Victor Hugo R. Coelho[b,]*, Yunqing Xuan[c], Davi de C. D. Melo[d], André N. Gadelha[a], Elias A. Santos Júnior[a], Carlos de O. Galvão[e], Geraldo M. Ramos Filho[a], Luis Romero Barbosa[a], George J. Huffman[f], Walt A. Petersen[g], Cristiano das N. Almeida[a]

[a] Department of Civil and Environmental Engineering, Federal University of Paraíba, João Pessoa, 58051-900, Brazil

[b] Department of Geosciences, Federal University of Paraíba, João Pessoa, 58051-900, Brazil

[c] College of Engineering, Swansea University, Bay Campus, Swansea, SA1 8EN, UK

[d] Department of Soils and Rural Engineering, Federal University of Paraíba, Areia, 58397-000, Brazil

[e] Technology and Natural Resources Centre, Federal University of Campina Grande, Campina Grande, 58429-900, Brazil

[f] NASA Goddard Space Flight Center, Greenbelt, MD 20771, USA

[g] NASA Marshall Space Flight Center, Huntsville, AL 35805, USA

***** Corresponding author. Tel.: +55-83-3216-7684.

E-mail address: victor.coelho@academico.ufpb.br (V.H.R. Coelho)

ABSTRACT: Sub-daily rainfall information is essential for many hydrological applications, but ground-based data availability is still an issue in poorly gauged regions worldwide. Satellite remote sensing missions, such as the Global Precipitation Measurement (GPM) mission, have been playing a key role in estimating sub-daily rainfall data globally. However, the quality of such information needs to be carefully evaluated. Previous studies evaluating sub-daily data from the Integrated multi-satellitE Retrievals for GPM (IMERG) product considered only the rainfall depth over pre-defined periods (e.g., hourly or half-hourly), with no analysis of the ability and quality of the product in defining the actual rainfall events and the associated properties. Thus, the objective of this study is to evaluate the performance of the IMERG Final Run Version

Accepted Manuscript by Journal of Hydrology. Published version aviable at
https://doi.org/10.1016/j.jhydrol.2020.125128

06B (V06B) product in capturing sub-daily rainfall events and their properties (depth, duration and intensity) over Brazil. The analysis consisted of comparing the satellite estimates against the ground-based data from 1,757 sub-daily rainfall gauges for a period of three years (2015–2017). This study used the minimum inter-event time (MIT) criterion to define independent rainfall events determined by dry periods: 1, 6 and 24 hours. Results show that IMERG can properly estimate the sub-daily rainfall depth for the three MITs considered, with the best results found in the southern part of the country. This means that the IMERG product represents a good source of sub-daily rainfall depth data for hydrological and hydroclimatic applications in Brazil. On the other hand, the evaluation shows large overestimations and underestimations of the IMERG product for rainfall duration and intensity properties, respectively. The results obtained from this study provide a reference for IMERG users who require sub-daily rainfall data based on events and further knowledge about its properties.

Keywords: GPM, evaluation, Inter-event time, Depth, Intensity, Duration.

1. Introduction

Rainfall is one of the main components of the hydrological cycle and its accurate quantification is fundamental to providing primary information for understanding and predicting some regional physical processes such as floods, landslides, soil erosion and severe storms (Kidd et al., 2017; Skofronick-Jackson et al., 2017). Sub-daily rainfall data are necessary for quantifying the characteristics of extreme events that trigger the physical processes mentioned above (Blenkinsop et al., 2018; Guerreiro et al., 2018; Lewis et al., 2019, 2018). Therefore, for hydrological application, dividing the rainfall into events is essential for a better understanding of such processes. For instance, Dunkerley (2012) showed that the rain event profile influences the partitioning of rainfall into ponding, infiltration and runoff.

Sub-daily rain event properties are also important for quantifying the soil erosion. For instance, this information is indispensable to the Universal Soil Loss Equation (USLE) and Revised Universal Soil-Loss Equation (RUSLE) developed by Wischmeier and Smith (1978) and Renard et al. (1997), respectively. Both the USLE and RUSLE equations are based on the so-called rainfall erosivity index, which is calculated with the maximum rainfall intensity during the 30-min period. The delineation of individual rain events is also the first step to generate the hyetographs for analysing the spatiotemporal variability of rainfall (Barbosa et al., 2018; Coutinho et al., 2014; Dolšak et al., 2016). Moreover, the development of robust Intensity-Duration-Frequency (IDF) curves for extreme rainfall studies, which are the key to many engineering designs, is sometimes interfered with by sparse, infrequent or short-record sub-daily observations in many locations (Courty et al., 2019; Lumbroso et al., 2011). Therefore, rain event properties are particularly relevant for studies related to hydrological and ecological processes (Haile et al., 2012; Molina-Sanchis et al., 2016).

As revealed by Dunkerley (2008a), most reported studies of rainfall event data regarded a fixed rainless period (a minimum inter-event time, MIT) as the common criterion to define events. The use of the MIT criterion is important for analysing the relationship between the yield of catchments (e.g., water, sedimentation and nutrients) and the rainfall events with regards to their properties (e.g., depth, duration, intensity, dry time and intermittency). Moreover, adopting a fixed time interval (hourly or 30 minutes) to define rainfall events is not appropriate because such an interval may encompass different events or part of one rainfall event; hence the MIT criteria provides a better way to recognise and understand single rainfall events. According to Dunkerley (2008a), the common values of MIT used for defining rainfall events varies between 3-min and 24-h. Following this, Dunkerley (2015, 2010, 2008a) carried out a series of studies in Australia to understand the influence of the MIT criterion on the rainfall event and its properties. These studies showed that longer MITs yield rainfall events with lower intensity, and conversely, longer MITs yield larger depth and duration. Similar studies highlighting the influence of the MIT criterion on the rainfall properties have been reported in other countries, e.g. see Haile et al. (2011); Medina-Cobo et al. (2016); Meier et al. (2016) and Molina-Sanchis et al. (2016).

However, characterising the sub-daily rainfall variability over large areas by in-situ data is still difficult because such records sparsely cover the entire global landmass, never mind the key tropical regions (Hegerl et al., 2015). The lack of sub-daily in-situ rainfall data is probably due to the higher implementation costs of rain gauges able to measure sub-daily events, compared with those that measure on a daily time-scale. Blenkinsop et al. (2018) identified more than 23,000 sub-daily gauges worldwide providing freely available rainfall data, with 60% of them concentrated in five countries: the United States (7,197), Australia (1,882), United Kingdom (1,869), Japan (1,723) and Germany (1,011). Countries from Africa and Latin America have the lowest availability of sub-daily data. For instance, at the time, they have identified only 45 rain gauges with sub-daily freely available rainfall data in Brazil. Consequently, rain rates, event durations and other rainfall properties at sub-daily time-scales have not been properly studied and are still poorly understood in such low-density gauge areas (Blenkinsop et al., 2018; Dunkerley, 2008b; Westra et al., 2014).

During the last few decades, the use of cutting-edge satellite-borne remote sensing technology has played a crucial role in providing valuable distributed observations of water resources, including precipitation data at sub-daily temporal resolution (Famiglietti et al., 2015; Levizzani et al., 2018; O and Kirstetter, 2018). The remotely sensed precipitation products mainly rely on algorithms that combine the data observed from microwave and infrared sensors together with other ancillary ground-based data (Hou et al., 2001; Kidd and Levizzani, 2011). Launched in 1997, the Tropical Rainfall Measuring Mission (TRMM) was one of the first dedicated and arguably most important satellites for obtaining information about precipitation in the latitude band 50° North and 50° South (Huffman et al., 2007). The TRMM Multi-satellite Precipitation Analysis (TMPA) dataset provides rainfall data at 0.25° spatial resolution and 3-hour temporal resolution. Several studies evaluated the performance of the TMPA products in many countries (e.g., Baik and Choi, 2015; Dembélé and Zwart, 2016; Dinku et al., 2008; Fang et al., 2013; Naumann et al., 2012; Pombo and de Oliveira, 2015), including Brazil (e.g., Buarque et al., 2011; Collischonn et al., 2008; Franchito et al., 2009; Melo et al., 2015), but most of them are mainly focused on daily or coarser time-scale evaluation. Even fewer studies checked the ability of the TMPA products for sub-daily (3-hour) applications such as flood forecasting (e.g., Nikolopoulos et al., 2013; Yuan et al., 2019). Specifically in Brazil, the studies evaluating the sub-daily performance of the TMPA products only used a few rain gauges at small and medium river basin scale (e.g., Laverde-Barajas et al., 2018).

After nearly two decades of many successful applications of TRMM, its successor, the Global Precipitation Measurement (GPM) mission launched its Core Observatory in 2014 and began to provide rainfall and snowfall information globally with better temporal (half-hour) and spatial (0.1° x 0.1°) resolutions, via the Integrated Multi-satellitE Retrievals for GPM (IMERG) products (Skofronick-Jackson et al., 2018, 2017). Due to the improvement in its resolution and enhancements for detecting light rain compared with the TMPA, IMERG opens up new opportunities for sub-daily applications of rainfall data for many purposes (Asong et al., 2017). Three IMERG products are currently available; depending on the time that the data becomes available to the end-users and the amount of information incorporated to improve the satellite estimations, they are referred to as the Early Run, Late Run and Final Run (Huffman et al., 2017). The Early and Late Run products are available at 4 and 12 h after observation, respectively, while the Final Run product is available 3.5 months after observation.

During the last five years, several studies have been carried out to evaluate the IMERG products in regions with different geographical characteristics worldwide, most of which present good agreement with the gauge and ground-based radar data (e.g., Asong et al., 2017; Li et al., 2018; O et al., 2017; O and Kirstetter, 2018; Prakash et al., 2018; Satgé et al., 2019, 2017; Tan et al., 2017; Tan and Duan, 2017; Tang et al., 2016b, 2016a, 2018; Wang et al., 2018). Some studies were conducted in Brazil assessing the quality of the IMERG products from different approaches at local-to-national scales (e.g., Gadelha et al., 2019; Lelis et al., 2018; Oliveira et al., 2018, 2016; Rozante et al., 2018; Salles et al., 2019). However, all studies performed in Brazil compared the IMERG estimates against ground-based data at relatively coarse temporal scales (daily or longer) when compared with the capability of the satellite-based product in detecting rainfall at a higher temporal resolution (half-hour). Moreover, worldwide, most studies that have assessed the IMERG data considered only the rainfall depth over pre-defined periods (Li et al., 2018; Tang et al., 2016a), with no analysis of the ability and quality of the product in defining the actual rainfall events (e.g., based on the MIT criterion) and the associated properties (rainfall depth, duration and intensity). Such analysis, which is essential for further applications of sub-daily data to predict the physical processes previously mentioned, is now possible thanks to the higher temporal resolution of the IMERG products. Furthermore, a more comprehensive and robust validation of the IMERG products in estimating the number of rain events and its properties can be done.

Considering the importance of high-quality sub-daily distributed rainfall data, the aims of this study are: (i) evaluating the performance of the IMERG product at sub-daily time-scale, (ii) analysing the potential of IMERG for delineating rainfall events and defining their properties (rainfall depth, duration and intensity), and (iii) identifying how the quality of the IMERG product is affected by the choice of MIT criterion (e.g., over 1, 6, and 24 h). Based on these aims, this study addresses the following scientific questions: (a) How does IMERG perform at sub-daily time-scale? (b) Is the IMERG product able to delineate rainfall events and define their properties for sub-daily applications? (c) Is the quality of IMERG affected by the choice of MIT criteria and rainfall regimes? This study intends to be a reference for sub-daily analysis of the IMERG product, covering a large-scale area that encompasses a variety of climate zones, rainfall patterns and terrains.

2. Materials and methods

2.1. Study area

This study was carried out in Brazil, a continental-wide country covering approximately 8.5 M km² encompassed by 5°16′N-33°45′S and 34°47′W-73°59′W (Fig. 1). Officially, the Brazilian territory is divided into five geographical regions, namely: South (S), Southeast (SE), Central-West (CW), North-East (NE), and North (N). Brazil is the largest country in the Southern Hemisphere in area, encompassing different climate zones and rainfall patterns due to its vast territory. According to the detailed analysis performed by Alvares et al. (2013), the Brazilian territory has twelve Köppen's climate types divided into three main zones (Tropical, Semiarid and Humid Subtropical), with a mean annual air temperature ranging approximately from 10 °C to 26 °C. It has five different rainfall regimes that do not fit very well with the geographical regions (Reboita et al., 2010; Rozante et al., 2018). The annual rainfall in Brazil is characterised by high spatial variability, with values ranging from 380 (semiarid in the NE) to 4,000 mm (tropical rainforest in the N) (Alvares et al., 2013; Gadelha et al., 2019; Melo et al., 2015). The rainfall regimes defined by Reboita et al. (2010) are described in Table 1.

INSERT FIG. 1 HERE

Fig. 1. (a) Selected rain gauges used as ground truth observations in this study and Köppen's classification map for Brazil according to Alvares et al. (2013). (b) Selected cells grouped according to homogenous rainfall characteristics (Section 2.6). The climatic symbol labels A, B and C stand for Tropical, Dry, and Humid Subtropical, respectively.

INSERT TABLE 1 HERE

Table 1. Summary of relevant characteristics of each homogeneous rainfall group, including the rainfall regimes defined by Reboita et al. (2010).

2.2. Observed rainfall data

This study began by considering rainfall data from 3,432 automated rain gauges distributed throughout the five official geographical regions in Brazil. The ground-based data for the period 1 January 2015 to 31 December 2017 were acquired from tipping bucket gauges with a 10-min temporal resolution when it rains and 60 min over no-rain periods. These rain gauges are operated by the Brazilian Centre for Monitoring and Early Warnings of Natural Disasters (CEMADEN) as part of a national-wide network that was established by the Brazilian Government in 2011 to support its natural disasters risk management (Horita et al., 2017). Unfortunately, the distribution of the rain gauges is rather uneven, with the largest portion concentrated along the Brazilian coastal region where the population density is also high. Thus, most rain gauges obtained from the CEMADEN network are located within the cities. The SE region, where the São Paulo and Rio de Janeiro metropolitan regions are located, for example, is covered by 1,594 rain gauges, i.e. 46% of the total. In contrast, the number of rain gauges in the N region, where the Amazon rainforest is located, corresponds to 2% (only 66 gauges) of the entire network. Although uneven, this in-situ rainfall monitoring network operated by CEMADEN represents an advance for understanding sub-daily rainfall extremes in tropical regions, since this type of data is currently much less available in other countries from Africa and Latin America.

Sub-daily rainfall data are mostly maintained by national meteorological agencies, but a single agreed upon global approach for quality assessment and control of the gauge-based measurements is still unavailable, especially when considering large areas (Westra et al., 2014). Meanwhile, a range of standard and sophisticated procedures for rainfall quality assessment and control has been proposed and recommended. The commonly used standard methods involve some of the following procedures (Westra et al., 2014): (i) checks of the range of values, (ii) changes in values over subsequent measurements, (iii) difference analysis between neighbouring stations, (iv) comparisons to other data types, (v) checking the range of time aggregations, and (vi) identification of breakpoints in rainfall time-series.

The observed rainfall data used in this study were quality-controlled based on two steps for detecting possible rain gauge inconsistencies and selecting high-quality data. Firstly, a computational routine selected only rain gauges with less than 30-days of missing data along each civil analysed year considered in this study. Thereafter, all the rain gauges meeting this first restriction were visually inspected using some of the above-mentioned standard methods. The first standard method compared monthly and sub-daily rainfall data of the five nearest stations to verify large discrepancies between them. For this first analysis, the distances and the differences of altitude between the analysed rain gauge and the nearest stations were considered for identifying only rainfall patterns corresponding to their specific region. The range of values and changes over subsequent measurements were then analysed for each rain gauge to identify constant or null rainfall records that probably indicate gauge clogging. After the data quality check, a total of 1,757 rain gauges were used in this study for the comparison (Fig. 1a), i.e. almost half of the automated stations were discarded.

2.3. IMERG data

The IMERG Final Run (IMERG-F) is a Level 3 GPM product that combines microwave and infrared estimates from the GPM constellation (Huffman et al., 2017). It also incorporates monthly gauge observations from the Global Precipitation Climatology (GPCC) and other ancillary data to improve the satellite estimations. This study compared ground- and satellite-based data independently, since the rain gauges operated by CEMADEM are not used by GPCC. The IMERG-F product is available 3.5 months after observations, which is not suitable for time-sensitive applications. Instead, the IMERG-F product is more suitable for hydrological and climate modelling purposes given its better performance compared to near-real-time products (Tang et al., 2016a). The IMERG-F dataset provide rainfall and snowfall information at 0.1º x 0.1º (spatial) and half-hour (temporal) resolutions. More information about the IMERG-F product are described in detail by Huffman et al. (2017) and Skofronick- Jackson et al. (2018). Specifically, this study used the latest IMERG-F Version-06B, which presents several major changes when compared to the previous versions, such as: i) the inclusion of additional sensors (particularly in the TRMM era), ii) improvements to parent GPM products, iii) modifications to the satellite intercalibrations, and iv) refinements to the morphing component (Tan et al., 2019). The comparison between the IMERG-F product and the rain gauge dataset was performed in this study at the native 30-minute scale. The IMERG-F dataset used in this study covers the same period of the ground-based data, i.e. between 1 January 2015 and 31 December 2017.

2.4. Rainfall events definition and properties

Many approaches are available for delineating individual rainfall events (Molina-Sanchis et al., 2016). However, the use of fixed time intervals (e.g. hourly or half-hourly) to define rainfall events can sometimes be inappropriate, since such intervals may contain part of only one or sometimes more than one event; hence the MIT criteria provide a better way to recognise and understand single rainfall events. This study used the MIT to discriminate successive independent events by a defined dry period (Dunkerley, 2008a), as previously mentioned. Some studies define optimum values of MIT depending on the studied region (e.g., Medina-Cobo et al., 2016; Molina-Sanchis et al., 2016), while others reveal that the definition of MIT is associated with the application of the study (e.g., Aryal et al., 2007; Bracken et al., 2008; Cattan et al., 2006). According to Chin et al. (2016), short values of MIT are better used in local studies more sensitive to rainfall variation, whereas longer values of MIT are preferred for studies considering a whole weather system. Following this, a range of MITs, e.g. 1, 6 and 24 h, were chosen in this study to define rainfall events.

This study also analysed three important properties of the IMERG-F rainfall product: the depth, duration and intensity. A rainfall depth threshold of 2.5 mm for defining rain/no-rain was established for all analyses to exclude events deemed insignificant. Any IMERG-F and rain gauge rainfall events below this threshold were treated as zero. The temporal resolutions of rain gauges and IMERG-F used to define rainfall events are 10-min and 30-min, respectively. Therefore, these are the possible shortest rainfall event durations.

2.5. Comparison and evaluation procedures

Comparison between the IMERG-F and rain gauge data was based on a pairwise approach (Fig. 2a). Point-to-cell analysis was performed when there was only one rain gauge available inside the IMERG-F native cell. On the other hand, an average points-to-cell analysis was considered for IMERG-F grid cells containing more than one rain gauge. Satellite gridded data without any rain gauges at all within the cell were excluded from the analyses. As a result, in total, there are 1,065 grid cells of the IMERG-F product considered in this study for analyses.

INSERT FIG. 2 HERE

Fig. 2. Methodological chart showing (a) the cells of the IMERG product considered in the study and (b) the approaches adopted based on pairwise level for properties' mean values comparison, detection analysis and error magnitude analysis.

Three evaluation procedures (EP) were performed to assess the quality of the IMERG-F product in detecting the rainfall events and their properties for different MIT values (Fig. 2b). Firstly, the differences between the mean values of the properties of all rainfall events estimated by the IMERG-F product and observed by the rain gauges were checked. This is the first evaluation procedure (EP1), which makes use of the correlation coefficient (CC) and the mean relative absolute error (MRAE), considering both national- and group-scale means.

$$\mathrm{CC} = \frac{\sum_{i=1}^{n}(O_i - \bar{O})(E_i - \bar{E})}{\sqrt{\sum_{i=1}^{n}(O_i - \bar{O})^2} \cdot \sqrt{\sum_{i=1}^{n}(E_i - \bar{E})^2}} \tag{1}$$

$$\mathrm{MRAE} = \frac{100}{n}\sum_{i=1}^{n}\left|\frac{O_i - E_i}{O_i}\right| \tag{2}$$

where O is the value observed by the rain gauges, $\bar{O}$ is the mean observed values, E is the value estimated by the IMERG-F product, $\bar{E}$ is the mean estimated values, and n is the total number of compared pairs.

A second evaluation procedure (EP2) was applied to verify whether the actual rainfall events correspond to those detected by the satellites. EP2 uses the metrics related to rainfall events detection: (i) probability of detection (POD), which shows the fraction of rainfall events that are correctly detected by the IMERG-F product; (ii) false alarm ratio (FAR), which exhibits the fraction of events estimated by the IMERG-F product but not detected by the rain gauge, and (iii) critical success index (CSI), which measures the fraction of IMERG-F events correctly detected for the total number of observed and estimated rainfall events:

$$\mathrm{POD} = \frac{a}{a + c} \tag{3}$$

$$\mathrm{FAR} = \frac{b}{a + b} \tag{4}$$

$$\mathrm{CSI} = \frac{a}{a + b + c} \tag{5}$$

where a is the number of rainfall events simultaneously identified by both rain gauge and IMERG-F, b is the number of rainfall events observed by the satellite product but not so by the ground-based data, and c is the number of rainfall events detected by the rain gauges but not observed by the IMERG-F product. The values of POD, FAR and CSI range from 0 up to 1. The perfect score for POD and CSI is close to 1, while the desirable values for FAR are close to 0. The three metrics applied to compare the detection of rainfall events are traditionally used for a defined time-space (e.g., Gadelha et al., 2018; Prakash et al., 2018; Rozante et al., 2018; Tan and Duan, 2017; Tang et al., 2016a), which is not the case of this study. Therefore, a sequential approach containing three specific criteria was established to evaluate whether the estimated event is really the same as the observed: (i) if the rainfall events are 100% overlapped, (ii) if the rainfall events are overlapped by more than 50% or (iii) if the time lag between the centroids are lower than 2.5 times the MIT.

Only the events detected according to EP2 were subjected to a third evaluation procedure (EP3), which computes the average magnitude of deviations between satellite and ground-based properties of events. EP3 only includes the MRAE of each property.

In summary, the EPs adopted in this study make it possible to identify whether the rainfall events observed by the rain gauges are adequately estimated by the IMERG-F product, as follows: (i) good agreement of average rainfall properties, (ii) ability to detect the events, and (iii) conformity of detected events properties (Fig. 2b).

2.6. Analysis of the rain gauge network density

Differences between point-scale gauge measurements and areal satellite-based rainfall can affect the validation conclusions of the IMERG-F product. Interpolation approaches are the only options for transferring point-scale rainfall observations into areal estimates before they are compared with the grid-cells of the satellite-based data (Tian et al., 2018). Alternatively, pairwise comparisons conducted only in grid-cells containing at least one rain gauge can also be used (Asong et al., 2017; Tan and Duan, 2017; Yang et al., 2016). However, the reliability of both methods used to compare satellite-based products and rain gauge data is intrinsically linked to the density of the ground reference (Tang et al., 2018; Tian et al., 2018). In order to ensure the reliability of the results, the dependence of the IMERG-F performance on the density of the rain gauge network used in this study was also investigated. There were then four metrics applied to verify the deviations of rainfall magnitudes for the IMERG-F product according to different gauge densities available in this study. Such metrics include the bias (BIAS), the mean relative error (MRE), the MRAE presented in Eq. (2) and the root mean square error (RMSE):

$$\mathrm{BIAS} = \sum_{i=1}^{n} (E_i - O_i) \quad (6)$$

$$\mathrm{MRE} = \frac{\sum_{i=1}^{n} (E_i - O_i)}{O_i} \quad (7)$$

$$\mathrm{RMSE} = \frac{\sqrt{\sum_{i=1}^{n} (E_i - O_i)^2}}{n} \quad (8)$$

2.7. Definition of regions based on homogeneous rainfall characteristics

As previously mentioned, the Brazilian territory encompasses a variety of climate zones and rainfall regimes. Therefore, it is necessary to cluster the rain gauges and their corresponding grids of the IMERG-F product in regions with similar characteristics, prior to the proposed analyses. The k-means clustering algorithm was applied to define these regions with similar rainfall patterns (Carvalho et al., 2016). There were five groups defined in this study based on the number of rainfall regions established for the Brazilian territory by Reboita et al. (2010) and Rozante et al. (2018).

All rain gauges selected after the quality control process were used to define these homogeneous regions, as shown in Figure 1b. There were six different variables obtained from these rain gauges used to define the regions: (i) elevation, (ii) annual rainfall, (iii) number of rainfall events, (iv) mean rainfall depth, (v) mean duration, and (vi) mean intensity. For the last four variables, all three different MITs used for the analyses were also considered when defining the regions. However, before the clustering analysis, the number of variables was reduced using Principal Component Analysis (PCA) (Dyer, 1975; Ogallo, 1989; Singh, 2006).

3. Results and discussion

3.1. Representativeness of the point(s)-to-cell analysis

The point(s)-to-cell analysis applied in this study was performed using 1,750 rain gauges distributed throughout 1,065 grid cells of IMERG, which corresponds to an overall density network of 1.64 gauges per 100 km^2. This represents more than eight times the threshold of one gauge per 575 km^2 recommended by the World Meteorological Organisation (WMO) for the interior plane and undulating areas (WMO, 1994). The number of rain gauges per grid cell of IMERG available for this study ranged from 1 to 12, as shown in Table 2. Grid cells with densities lower than four rain gauges per 100 km^2 stand for more than 90% of the analysed pixels. Conversely, grid cells containing more than seven rain gauges represent less than 1% of the total pixels evaluated in this study. According to the review carried out by Tian et al. (2018), the rain gauge network used in this study is denser than in most other previous studies evaluating satellite-based rainfall products.

INSERT TABLE 2 HERE

Table 2. Rain gauge densities per grid cells used in this study.

Figure 3 shows the evaluation results of the metrics for all available rain gauge density networks. This evaluation also considers the three rainfall properties and MITs used in this study. Overall, it is not possible to identify an improvement of the evaluation performance with the increase of the gauge density. For instance, the BIAS of the rainfall depth and duration remained practically unchanged for the two shorter MITs considered in this study. In contrast, the results show that denser gauge networks tend to slight increase the values of RMSE for all MITs and rainfall properties. This result differs from the studies carried out by Tang et al. (2018) and Tian et al. (2018) that detected a strong dependence of the evaluating metrics for the IMERG product on the rain gauge densities. Tang et al. (2018) found 2.5 gauges per grid cell at 0.1° spatial scale as the more reliable density to accurately evaluate satellite precipitation products in a river basin in South China. However, they recommended that future studies should explore the sensitivity of the results to variations in topography, climate conditions and precipitation phase (solid or liquid) because this number can be influenced by the region and season. On the other hand, the study performed by Tian et al. (2018) found that the evaluation of the IMERG satellite product exhibited better accuracy for most metrics when considering one gauge or more per grid cell.

INSERT FIGURE 3 HERE

Fig. 3. Evaluation metrics for all rain gauge densities and Minimum Intra-event Times (MIT) used in this study. The symbols ME, MAE, BIAS and RMSE stand for mean error, mean absolute error, bias and root mean square error.

3.2. Homogenous rainfall groups

Fig. 1b shows the spatial distribution cells, separated by groups with homogenous rainfall characteristics, after the application of PCA and k-means clustering algorithm. Group 1 is mainly located in the N and NE regions of Brazil, containing 163 cells (Table 1). The main atmospheric systems that have influence on this group of cells with the same rainfall patterns are those in the Intertropical Convergence Zone (ITCZ) and the Mesoscale Convective Complex (MCC) (Cohen et al., 1995; Espinoza Villar et al., 2009). According to Köppen's classification proposed by Alvares et al. (2013), the climates of the region where Group 1 is placed are tropical monsoon (Am) and tropical with dry winter (Aw), with an average annual temperature of 26 °C. The annual mean rainfall in the Group 1 ranges from 1,400 to 2,000 mm, most of which is concentrated between January and May (Fig. 4a). Group 2 mostly encompass the cells located along the Atlantic coastal zone of Northeast Brazil, which is mainly characterised by the Instability Lines (IL) and Southeast Trade Winds (SETW) atmospheric systems (Kousky, 1988; Reboita et al., 2010). Group 2 presents a fewer number of evaluated cells in this study – 108 in total. The climate of this group is mainly tropical with dry summer (As), with historical mean rainfall ranging from 1,200 to 1,800 mm year^{-1} and mean monthly air temperature above 23 °C throughout the year (Fig. 4b). Most of the 209 cells of Group 3 are located in the region of the Southeast, mainly characterised by a tropical with dry summer (As) climate, with mean annual rainfall ranging from 1,000 to 1,300 mm and concentrating during the austral summer (Melo et al., 2015) (Fig. 4c). The main climate systems influencing Group 3 are the South Atlantic Subtropical Anticyclone (SASA) and the South Atlantic Convergence Zone (SACZ) (Reboita et al., 2010; Rozante et al., 2018), with the mean monthly air temperature varying between 18°C and 24 °C throughout the year. Groups 4 and 5 own the largest number of analysed cells in this study (317 and 268, respectively). Both groups are mainly located in the S and SE regions, with a humid subtropical climate (C). The South Atlantic Subtropical Anticyclone (SASA) and South Atlantic Convergence Zone (SACZ) are the main climate systems influencing the Group 4, while Group 5 is influenced more by the Prefrontal Squall Line (PSL) and Cold Fronts (CF) climate systems (Reboita et al., 2010; Velasco and Fritsch, 1987). The annual rainfall in the cells of Group 4 ranges between 1,300 and 1,900 mm, most of which is concentrated during the austral summer (Fig. 4d). In contrast, the rainfall is spatially more uniform throughout the year in Group 5, ranging from 1,600 to 2,200 mm (Fig. 4e). The monthly average air temperature in Group 5 ranges from 12 °C in July to 23 °C in January.

INSERT FIG. 4 HERE

Fig. 4. Long-term (1950–1990) mean monthly rainfall and mean air temperature of each group with homogenous rainfall characteristics, obtained from 891 meteorological stations used by Alvares et al. (2013).

3.3. Nation-wide mean values comparison of the properties of rainfall events

In this first analysis, the IMERG data were evaluated by comparing the mean property values of all rainfall events identified by MIT from both IMERG and rain gauge. Fig. 5 shows the scatter plots based on the mean values, considering all cells analysed for the entire country. The outliers were visually excluded from this figure for better visualisation of the point cloud. Overall, the comparison between the two data sources indicates that the IMERG product presented a good agreement with the rainfall depths observed by the rain gauges, with a solid blotch of points concentrated close to the line of equality for all considered MITs (Fig. 5a to c). The concentration of most of the points above the line can demonstrate a slight overestimation of the rainfall depth by the IMERG product for all individual events. Similar behaviour of slight overestimation was also observed by Rozante et al. (2018) and Gadelha et al. (2019) when evaluating the rainfall depth of IMERG over Brazil at coarser temporal scales (daily onward). Similar performance behaviour of the sub-daily mean areal precipitation from IMERG was also noticed in other large-scale studies carried out in different regions of the World (e.g., Li et al., 2018; Mayor et al., 2017; Tang et al., 2016a). The CC for the rainfall depth considering the cells of all groups ranged from 0.36 (MIT = 24h) to 0.66 (MIT = 6 h), with values of MRAE (< 32%) indicating low variability of data between the rain gauges and the IMERG product for all MIT. It is also noticeable that the mean rainfall depth progressively increased for both sources of data as MIT become greater, as observed in-depth by Dunkerley (2015), Medina-Cobo et al. (2016) and Molina-Sanchis et al. (2016) using only tipping-bucket rain gauge data.

INSERT FIG. 5 HERE

Fig. 5. Scatter plots of the mean gauge values vs IMERG-F categorised into columns (from the left to right: depth, duration and intensity) and rows (from the top to bottom, the following MIT: 1, 6 and 24 h). The shaded contours and the line plots along the top and right axes are joint and marginal distributions of the gauge and IMERG-F. CC and MRAE stand for correlation coefficient and mean relative error, respectively.

The mean duration and intensity, considering all analysed cells, show a poor agreement between the IMERG product with the observed rainfall data for all MITs (Fig. 5d to i). For the mean duration, a large overestimation of the satellite-based product was observed, with negative linear correlations with respect to the two longer MITs, i.e. 6 h (CC = -0.19) and 24 h (CC = -0.03). These negative and low values of linear correlations represent an absence of correlation when comparing the two different rainfall datasets. For the mean intensity, however, the IMERG products presented a large underestimation when compared with the observed data, showing almost all points concentrated below the line of equality and the CC values ranging from -0.29 to -0.49. This behaviour was expected because the mean intensity inversely correlates to the mean duration, as a well-known feature from the relationship between intensity, depth and duration (Dunkerley, 2008a). Overall, it is also noticeable that the mean durations of IMERG present far larger amplitudes of data, with values up to three times higher than that observed in the rain gauges. Accordingly, the mean observed intensity is inversely proportional to the MIT, with amplitudes of values reducing significantly when rain events are longer, as also noticed and analysed by Dunkerley (2015) in Australia. In contrast, the mean intensity estimated by the IMERG product exhibits low dispersion for all MITs, with minimum and maximum values of 0.2 (MIT = 24 h) and 2.5 mm h-1 (MIT = 1 h), respectively. The MRAE values vary widely from 141 to 213% for mean duration and from 55 to 69% for mean intensity. The disagreement detected for the rainfall intensity occurs because the IMERG-F product is adjusted so that the monthly rainfall depth matches up with the rain gauges represented in the GPCC analysis (Becker et al., 2013; Schneider et al., 2014). This calibration does not affect the duration of the satellite event, so the intensity will be adjusted to whatever it takes over the duration of the event to fit the total monthly rainfall.

This analysis considering national-wide mean values comparison can lead to a false conclusion when data from the various regions are evaluated in a single pool. Therefore, the following sections present the results based on the comparison of homogenous rainfall groups.

3.4. Homogenous group-wide mean values comparison of the properties of event

Fig. 6 shows the box plots of the mean values for all analysed rainfall properties, separated by groups with homogenous characteristics, with extreme values also visually excluded for better visualisation of the data. Overall, the rainfall depth estimated by the IMERG-F product shows similar distribution with the data obtained from the rain gauges for all groups, with groups 3, 4 and 5 having the closest patterns. There is a slight overestimation in the satellite-based product compared with the observed data for all MITs. In contrast, Groups 1 and 2 exhibited the worst performance considering longer (24 h) and shorter (1 and 6 h) enclosing rain events, respectively. Rozante et al. (2018) and Gadelha et al. (2019) also noted low performance of IMERG-F in capturing daily rainfall depth in regions where the Groups 1 and 2 are predominantly located. The best CCs for rainfall depth were observed for Group 1, with values equal to or higher than 0.52 for all MITs (Table 3). Although presenting the best CC values, the variability of data between IMERG and rain gauges was substantially high for MITs equal to 24 h in Group 1, with MRAE reaching values higher than 90%. The reduction of the number of events registered by IMERG-F for longer MIT probably influenced the increase of the mean rainfall depth and, consequently, the values of MRAE in Group 1. This effect may be caused by the influence of convective clouds that prevail in this group, since this type of cloud can be falsely detected by the infrared sensors of the satellite, as also noticed by Rozante et al. (2018) and Gadelha et al. (2019). Overall, Groups 4 and 5 presented the lowest variabilities of the mean rainfall depth between the two sources of data (MRAE < 30%), independently of the MIT considered.

INSERT FIG. 6 HERE

Fig. 6. Box plots of the mean gauge values and IMERG-F for the five homogenous rainfall groups, categorised into columns (from the left to right: depth, duration and intensity) and rows (from top to the bottom, the following MIT: 1, 6 and 24 h).

INSERT TABLE 3 HERE

Table 3. Summary of evaluation metrics for the IMERG-F product, considering the mean values of rainfall properties for each homogeneous group.

The mean duration of the events from the IMERG-F product is significantly overestimated compared with that of the ground-based data for all five homogenous groups (Fig. 6d to f), following the same characteristics observed for the national-scale mean comparison. Similarly, for the rainfall depth, Group 1 has the worst performance in terms of using the IMERG-F in detecting the mean duration, with values of MRAE higher than 300% for all MITs considered in this study (Table 3). The best performance of the IMERG-F in identifying the duration of the gauge data was observed in Group 5 (54% < MRAE < 150%), although the values of CC showed negative correlations for the two shorter MITs. Such performance is most likely caused by the prevalence of rainfall from Cold Front weather systems with low intensity and long durations, as noted by Rozante et al. (2018). In general, the shorter MIT of the IMERG-F dataset represented the mean duration of the rain gauges worse regardless of the homogenous rainfall group (150% < MRAE < 322%). These behaviours show that the IMERG-F product can adequately capture the rainfall depth but with longer duration when compared to the ground-based dataset. The durations of the satellite-based product result in a large underestimation of the rainfall intensity of IMERG-F. Once again, Group 1 exhibited the largest deviations and errors in the evaluation of the satellite rainfall product, with MRAE obtained for rainfall intensity exceeding 80% for all MIT. Conversely, lower errors for the rainfall intensity were found in Groups 2 and 5, although coming with high values of MRAE (from 37 to 58%) and low positive CC (< 0.43). This fact limits the use of the IMERG-F for those purposes that require accurate information about rainfall duration and intensity, such as soil loss (Medeiros and Araújo, 2014) and production of surface runoff (Figueiredo et al., 2016).

3.5. Mean values comparison of trends by fixed thresholds

This section evaluates the agreement of the mean values of all rainfall properties of the IMERG-F product according to the level of underestimation or overestimation, which is split into seven categories as shown in Fig. 7. Overall, the mean rainfall depth of IMERG-F exhibited low relative errors across all groups, especially for the two shorter MITs, where more than 50% of the cells showed a good agreement for almost all groups. An exception was noticed in Group 2, where a mix of moderate and slight overestimations prevailed in more than 50% of the cells. A reduction in the number of cells presenting good agreement was observed in almost all homogenous groups for longer MIT values, except in Group 2. This effect was caused by the aggregation of individual rain events that increased the rainfall depth in longer MITs, as deeply discussed by Dunkerley (2008a). In this study, the increase of rainfall depth within longer rain events was more accentuated for the IMERG-F product when compared to the observed dataset, which is evidenced by the considerable number of cells presenting slight and moderate overestimations in all groups. Group 1 concentrates the largest relative errors for the longer MIT, with moderate and large overestimations representing more than 75% of the cells in this group.

INSERT FIG. 7 HERE

Fig. 7. Stacked bars of the relative errors for the five homogenous rainfall groups. The charts are organised into columns referring to the rainfall property (from left to right: depth, duration, and intensity) and rows referring to the MIT (from the top to bottom: 1, 6 and 24 h).

Generally, the IMERG-F product is unable to successfully represent the mean rainfall duration or intensity of the events observed by the rain gauges, with most cells displaying large overestimations and underestimations mainly for shorter MITs, respectively (Fig. 7d to i). The performance of the group 1 does not practically change across different MITs when comparing duration and intensity. Group 1 demonstrates very large deviations in duration (overestimation) and intensity (underestimation). On the other hand, Group 2 exhibited a better performance of rainfall duration and intensity, with approximately 30% of the analysed cells deemed to be in 'good agreement' for the two longer MITs. This analysis confirms the results found in the previous sections that indicate a limitation of the IMERG-F product to represent the intensity and duration of the same sub-daily rainfall events observed by the gauges but with complementary information regarding the percentage of cells in each homogenous group according to the agreement thresholds.

3.6. Analysis of rainfall events detection

The results presented in the previous sections show a good agreement between the mean rainfall depth estimated by the IMERG-F product and observed by the ground-based dataset, which was not noted for the two other rainfall properties (duration and intensity). This section analyses if the IMERG-F product is able to accurately match the same rainfall events detected by the rain gauges. Fig. 8 shows considerable improvement of the IMERG-F product performance in detecting ground-based rainfall events as MIT increases. An exception was noticed in Group 1, where more events were correctly detected for the MIT of 6 h. Overall, Groups 4 and 5 presented the highest POD values for all MIT, ranging from ~0.3 (MIT = 1 h) to ~0.8 (MIT = 24h). The results exhibited in Fig. 8a indicate a good skill of IMERG-F in detecting individual rain events equal to or higher than 6 h in those two groups located in Southern Brazil, as also noted by Lelis et al. (2018) and Gadelha et al. (2019) in their evaluation of the IMERG-F product from daily to annual time-scales. This performance of POD is corroborated by the distribution of CSI, which followed the same characteristics but with lower values due to the high number of detected FAR. Similar behaviour was also observed by Tang et al. (2016a) who assessed the IMERG-F product in China, where POD presented values ~20% larger than CSI. On the other hand, Groups 1 and 2 displayed POD values lower than 0.5 for the longer MIT. Rozante et al. (2018) also observed low detection of IMERG-F along the Atlantic coast of NE Brazil, where most of Group 2 is located, even considering analyses on a monthly basis. Unlike POD and CSI, the

FAR presented an inverse relation with the MIT, with the highest false alarms observed for rain events equal to 1 h in all groups. The FAR exhibited similar performance for all groups, with the largest proportional reduction of false alarms identified between the two shorter MITs.

INSERT FIG. 8 HERE

Fig. 8. Spider chart representing (a) the probability of detection (POD), (b) the false alarm ratio (FAR) and (c) the critical success index (CSI) for all homogeneous rainfall groups and Minimum Intra-event Times (MIT). The symbols G1, G2, G3, G4 and G5 stand for group 1, group 2, group 3, group 4 and group 5, respectively.

3.7. Error magnitude analysis

Results relative to EP2 are depicted by the spider charts assessing the magnitude of deviations between the rainfall properties estimated by the IMERG-F product and observed by the rain gauges (Fig. 9). The MRAE values presented a general behaviour of remaining unchanged with the aggregation of the rainfall depth events in almost all groups, with values close to 100%. Only Group 2 exhibited an increase in the magnitude of the depth error when longer no-rain periods are included within rainfall events. Gadelha et al. (2019) also found large deviations of rainfall depth in most cells located in the coastal zone of the Brazilian NE when evaluating the IMERG-F product on coarser time-scales. Such poor performance was attributed by the authors to the warm-rain process-dominated systems that are not well detected by the passive microwave sensors over land. The values of MRAE for duration follow the general pattern observed in the rainfall depth but with higher errors also detected in Group 2, especially for the MIT = 24 h (> 600%). The largest values of MRAE were noticed for rainfall intensity, wherein the deviations of IMERG-F range from 300 (Group 5) to 2,000% (Group 1) for the longer MIT.

INSERT FIG. 9 HERE

Fig. 9. Spider charts representing the mean relative absolute error (MRAE) for (a) rainfall depth, (b) rainfall duration and (c) rainfall intensity of all homogeneous groups and Minimum Intra-event Time (MIT). The abbreviations are the same as in Figure 8.

4. Summary and conclusions

This study is the first national-scale assessment of the IMERG-F product at sub-daily temporal resolution in Brazil. Moreover, the analyses focused on the potential of the satellite-based data in delineating rainfall events and defining some of its properties, such as depth, duration and intensity. The evaluation was carried out using 1,065 grid cells of the IMERG-F product, separated into five different groups with homogenous rainfall characteristics. The main specific findings of this study are summarised as follows:

(1) The IMERG-F product exhibited good performance in capturing the rainfall depth for all MITs considered in this study, with some variations depending on the analysed group. Overall, the rainfall depth estimated by the satellite product presented better performance in cells located in southern Brazil, specifically in Groups 4 and 5.

(2) IMERG-F presented a slight tendency in overestimation the ground-based rainfall depth data for all MITs. This overestimation tends to slightly increase when longer rain events are analysed, although a considerable improvement of the probability of detection was also noticed when more rain events were incorporated.

(3) The evaluations revealed large overestimations and underestimations of the IMERG-F product for rainfall duration and intensity, respectively. This behaviour was noted for all groups and all MITs probably because i) the calibration of the IMERG-F product that is made to match the monthly rain gauges rainfall depth incorporated to improve the satellite estimates, and ii) the capability of the microwave and infrared sensors for identifying rain/no-rain. In general, these sensors detect longer rainfall events than those that actually occurred. Such finding limits the use of the IMERG-F product in Brazil for some applications that require rainfall intensity and duration information with high temporal resolution.

(4) The analyses reveal that the detection of events by the IMERG-F product tends to improve with the increasing of MIT. However, the rainfall properties remain not well-represented with this improvement, especially the intensity and duration.

(5) Overestimations and underestimations of the IMERG-F product were more evident in regions with the presence of Mesoscale Convective Systems (Group 1). On the other hand, in regions with

the presence of Cold Front weather systems and rainfall characterised by long duration and low intensity, the IMERG-F product better estimated the sub-daily rainfall data (Group 5).

The results obtained from this study provide a reference for IMERG-F V06B use cases that require sub-daily rainfall data based on events and further knowledge about its properties. Based on our findings, the sub-daily information on rainfall depth from the IMERG-F product can be a good source of data for hydroclimatic and hydrological studies in Southern Brazil. On the other hand, sub-daily rainfall depth data from the IMERG-F product have to be carefully checked when used throughout the NE coastal region because of the larger overestimations and underestimations associated with the weather systems (IL and SETW) and the reduced capability of the sensor to detect some precipitation and cloud types. Unfortunately, the number of rain gauges with sub-daily data from the CEMADEN network is limited over the N region where the Amazon rainforest is located, which makes a more accurate assessment of the IMERG-F product in this area difficult. Finally, this study highlights the need for further analyses event-by-event in each cell of the IMERG-F product to verify the influence of the hydroclimatic variables in the detection of rainfall intensity and duration events. Moreover, improvements in rainfall intensity and duration estimates of the IMERG-F product are necessary for better identification of rain/no-rain, since the generation of a rainfall event, however small it is, leads to a change of the duration and, consequently, the intensity.

Acknowledgements: The Brazilian and British authors would like to acknowledge the financial support from the Brazilian National Council for Scientific and Technological Development (CNPq) for funding the Universal MCTI/CNPq No. 28/2018 (Grant REF: 433801/2018-2). This study was also financed in part by the Coordenação de Aperfeiçoamento de Pessoal de Nível Superior (CAPES) – Finance Code 001. The NASA authors were funded under the Precipitation Measurement Missions and Global Precipitation Measurement (GPM) mission projects. The British author was also supported by the Fundação de Apoio à Pesquisa do Estado da Paraíba (FAPESQ-PB), in partnership with the Newton Fund, via CONFAP – The UK Academies Research Mobility 2017/2018 (Grant REF: 039/2018). Special thanks are given to CEMADEM (Brazilian Centre for Monitoring and Early Warnings of Natural Disasters) for providing the rainfall database used in this study. Finally, we acknowledge the three anonymous reviewers and the editors for the constructive comments that improved a lot the quality of the manuscript.

References

Alvares, C.A., Stape, J.L., Sentelhas, P.C., De Moraes Gonçalves, J.L., Sparovek, G., 2013. Köppen's climate classification map for Brazil. Meteorol. Zeitschrift 22, 711–728. https://doi.org/10.1127/0941-2948/2013/0507

Aryal, R.K., Furumai, H., Nakajima, F., Jinadasa, H., 2007. The role of inter-event time definition and recovery of initial/depression loss for the accuracy in quantitative simulations of highway runoff. Urban Water J. 4, 53–58. https://doi.org/10.1080/15730620601145873

Asong, Z.E., Razavi, S., Wheater, H.S., Wong, J.S., 2017. Evaluation of Integrated Multisatellite Retrievals for GPM (IMERG) over Southern Canada against ground precipitation observations: A preliminary assessment. J. Hydrometeorol. 18, 1033–1050. https://doi.org/10.1175/JHM-D-16-0187.1

Baik, J., Choi, M., 2015. Spatio-temporal variability of remotely sensed precipitation data from COMS and TRMM: Case study of Korean peninsula in East Asia. Adv. Sp. Res. 56, 1125–1138. https://doi.org/10.1016/j.asr.2015.06.015

Barbosa, L.R., Almeida, C. das N., Coelho, V.H.R., Freitas, E. da S., Galvão, C. de O., de Araújo, J.C., 2018. Sub-hourly rainfall patterns by hyetograph type under distinct climate conditions in Northeast of Brazil: a comparative inference of their key properties. Rev. Bras. Recur. Hídricos 23. https://doi.org/http://dx.doi.org/10.1590/2318-0331.231820180076

Becker, A., Finger, P., Meyer-Christoffer, A., Rudolf, B., Schamm, K., Schneider, U., Ziese, M., 2013. A description of the global land-surface precipitation data products of the Global Precipitation Climatology Centre with sample applications including centennial (trend) analysis from 1901–present. Earth Syst. Sci. Data 5, 71–99. https://doi.org/10.5194/essd-5-71-2013

Blenkinsop, S., Fowler, H.J., Barbero, R., Chan, S.C., Guerreiro, S.B., Kendon, E., Lenderink, G., Lewis, E., Li, X.-F., Westra, S., Alexander, L., Allan, R.P., Berg, P., Dunn, R.J.H., Ekström, M., Evans, J.P., Holland, G., Jones, R., Kjellström, E., Klein-Tank, A., Lettenmaier, D., Mishra, V., Prein, A.F., Sheffield, J., Tye, M.R., 2018. The INTENSE project: using observations and models to understand the past, present and future of sub-daily rainfall extremes. Adv. Sci. Res. 15, 117–126. https://doi.org/10.5194/asr-15-117-2018

Bracken, L.J., Cox, N.J., Shannon, J., 2008. The relationship between rainfall inputs and flood generation in south–east Spain. Hydrol. Process. 22, 683–696. https://doi.org/10.1002/hyp.6641

Buarque, D.C., De Paiva, R.C.D., Clarke, R.T., Mendes, C.A.B., 2011. A comparison of Amazon rainfall characteristics derived from TRMM, CMORPH and the Brazilian national rain gauge network. J. Geophys. Res. Atmos. 116, 1–12. https://doi.org/10.1029/2011JD016060

Carvalho, M.J., Melo-Gonçalves, P., Teixeira, J.C., Rocha, A., 2016. Regionalization of Europe based on a K-Means Cluster Analysis of the climate change of temperatures and precipitation. Phys. Chem. Earth, Parts A/B/C 94, 22–28. https://doi.org/10.1016/j.pce.2016.05.001

Cattan, P., Cabidoche, Y., Lacas, J., Voltz, M., 2006. Effects of tillage and mulching on runoff under banana (Musa spp.) on a tropical Andosol. Soil Tillage Res. 86, 38–51. https://doi.org/10.1016/j.still.2005.02.002

Chin, R.J., Lai, S.H., Chang, K.B., Jaafar, W.Z.W., Othman, F., 2016. Relationship between minimum inter-event time and the number of rainfall events in Peninsular Malaysia. Weather 71, 213–218. https://doi.org/10.1002/wea.2766

Cohen, J.C.P., Silva Dias, M.A.F., Nobre, C.A., 1995. Environmental conditions associated with Amazonian Squall Lines: A case study. Mon. Weather Rev. 123, 3163–3174. https://doi.org/10.1175/1520-0493(1995)123<3163:ECAWAS>2.0.CO;2

Collischonn, B., Collischonn, W., Tucci, C.E.M., 2008. Daily hydrological modeling in the Amazon basin using TRMM rainfall estimates. J. Hydrol. 360, 207–216. https://doi.org/10.1016/j.jhydrol.2008.07.032

Courty, L.G., Wilby, R.L., Hillier, J.K., Slater, L.J., 2019. Intensity-duration-frequency curves at the global scale. Environ. Res. Lett. 14, 084045. https://doi.org/10.1088/1748-9326/ab370a

Coutinho, J. V, Leal, A.M.F., Almeida, C.N., Barbosa, L.R., 2014. Characterization of sub-daily rainfall properties in three raingauges located in northeast Brazil. Proc. Int. Assoc. Hydrol. Sci. 364, 345–350. https://doi.org/10.5194/piahs-364-345-2014

Dembélé, M., Zwart, S.J., 2016. Evaluation and comparison of satellite-based rainfall products in Burkina Faso, West Africa. Int. J. Remote Sens. 37, 3995–4014. https://doi.org/10.1080/01431161.2016.1207258

Dinku, T., Chidzambwa, S., Ceccato, P., Connor, S.J., Ropelewski, C.F., 2008. Validation of high- resolution satellite rainfall products over complex terrain. Int. J. Remote Sens. 29, 4097–4110.

https://doi.org/10.1080/01431160701772526

Dolšak, D., Bezak, N., Šraj, M., 2016. Temporal characteristics of rainfall events under three climate types in Slovenia. J. Hydrol. 541, 1395–1405. https://doi.org/10.1016/j.jhydrol.2016.08.047

Dunkerley, D., 2015. Intra-event intermittency of rainfall: An analysis of the metrics of rain and no-rain periods. Hydrol. Process. 29, 3294–3305. https://doi.org/10.1002/hyp.10454

Dunkerley, D., 2012. Effects of rainfall intensity fluctuations on infiltration and runoff: Rainfall simulation on dryland soils, Fowlers Gap, Australia. Hydrol. Process. 26, 2211–2224. https://doi.org/10.1002/hyp.8317

Dunkerley, D., 2010. How do the rain rates of sub-event intervals such as the maximum 5-and 15-min rates (I5 or I30) relate to the properties of the enclosing rainfall event? Hydrol. Process. 24, 2425–2439. https://doi.org/10.1002/hyp.7650

Dunkerley, D., 2008a. Identifying individual rain events from pluviograph records: a review with analysis of data from an Australian dryland site. Hydrol. Process. 22, 5024–5036. https://doi.org/10.1002/hyp

Dunkerley, D., 2008b. Rain event properties in nature and in rainfall simulation experiments: A comparative review with recommendations for increasingly systematic study and reporting. Hydrol. Process. 22, 4415–4435. https://doi.org/10.1002/hyp.7045

Dyer, T.G.J., 1975. The assignment of rainfall stations into homogeneous groups: An application of principal component analysis. Q. J. R. Meteorol. Soc. 101, 1005–1013. https://doi.org/10.1002/qj.49710143020

Espinoza Villar, J.C., Ronchail, J., Guyot, J.L., Cochonneau, G., Naziano, F., Lavado, W., De Oliveira, E., Pombosa, R., Vauchel, P., 2009. Spatio-temporal rainfall variability in the Amazon basin countries (Brazil, Peru, Bolivia, Colombia, and Ecuador). Int. J. Climatol. 29, 1574–1594. https://doi.org/10.1002/joc.1791

Famiglietti, J.S., Cazenave, A., Eicker, A., Reager, J.T., Rodell, M., Velicogna, I., 2015. Satellites provide the big picture. Science (80-.). 349, 684–685. https://doi.org/10.1126/science.aac9238

Fang, J., Du, J., Xu, W., Shi, P., Li, M., Ming, X., 2013. Spatial downscaling of TRMM precipitation data based on the orographical effect and meteorological conditions in a mountainous area. Adv. Water Resour. 61, 42–50. https://doi.org/10.1016/j.advwatres.2013.08.011

Figueiredo, J.V., Araújo, J.C., Medeiros, P.H.A., Costa, A.C., 2016. Runoff initiation in a preserved semiarid

Caatinga small watershed, Northeastern Brazil. Hydrol. Process. 30, 2390–2400. https://doi.org/10.1002/hyp.10801

Franchito, S.H., Rao, V.B., Vasques, A.C., Santo, C.M.E., Conforte, J.C., 2009. Validation of TRMM precipitation radar monthly rainfall estimates over Brazil. J. Geophys. Res. Atmos. 114. https://doi.org/10.1029/2007JD009580

Gadelha, A.N., Coelho, V.H.R., Xavier, A.C., Barbosa, L.R., Melo, D.C.D., Xuan, Y., Huffman, G.J., Petersen, W.A., Almeida, C. das N., 2019. Grid box-level evaluation of IMERG over Brazil at various space and time scales. Atmos. Res. 218, 231–244. https://doi.org/10.1016/j.atmosres.2018.12.001

Gadelha, A.N., Coelho, V.H.R., Xavier, A.C., Barbosa, L.R., Melo, D.C.D., Xuan, Y., Huffman, G.J., Petersen, W.A., Almeida, C.N., 2018. Grid box-level evaluation of IMERG over Brazil at various space and time scales. Atmos. Res. https://doi.org/10.1016/j.atmosres.2018.12.001

Guerreiro, S.B., Fowler, H.J., Barbero, R., Westra, S., Lenderink, G., Blenkinsop, S., Lewis, E., Li, X.-F., 2018. Detection of continental-scale intensification of hourly rainfall extremes. Nat. Clim. Chang. 8, 803–807. https://doi.org/10.1038/s41558-018-0245-3

Haile, A.T., Habib, E., Elsaadani, M., Rientjes, T., 2012. Inter-comparison of satellite rainfall products for representing rainfall diurnal cycle over the Nile basin. Int. J. Appl. Earth Obs. Geoinf. 21, 230–240. https://doi.org/10.1016/j.jag.2012.08.012

Haile, A.T., Rientjes, T.H.M., Habib, E., Jetten, V., Gebremichael, M., 2011. Rain event properties at the source of the Blue Nile River. Hydrol. Earth Syst. Sci. 15, 1023–1034. https://doi.org/10.5194/hess-15-1023-2011

Hegerl, G.C., Black, E., Allan, R.P., Ingram, W.J., Polson, D., Trenberth, K.E., Chadwick, R.S., Arkin, P.A., Sarojini, B.B., Becker, A., Dai, A., Durack, P.J., Easterling, D., Fowler, H.J., Kendon, E.J., Huffman, G.J., Liu, C., Marsh, R., New, M., Osborn, T.J., Skliris, N., Stott, P.A., Vidale, P.-L., Wijffels, S.E., Wilcox, L.J., Willett, K.M., Zhang, X., 2015. Challenges in quantifying changes in the global water cycle. Bull. Am. Meteorol. Soc. 96, 1097–1115. https://doi.org/10.1175/BAMS-D-13-00212.1

Horita, F.E.A., de Albuquerque, J.P., Marchezini, V., Mendiondo, E.M., 2017. Bridging the gap between decision-making and emerging big data sources: An application of a model-based framework to disaster management in Brazil. Decis. Support Syst. 97, 12–22. https://doi.org/10.1016/j.dss.2017.03.001

Hou, A.Y., Zhang, S.Q., da Silva, A.M., Olson, W.S., Kummerow, C.D., Simpson, J., 2001. Improving global analysis and short–range forecast using rainfall and moisture observations derived from TRMM and SSM/I passive microwave sensors. Bull. Am. Meteorol. Soc. 82, 659–679. https://doi.org/10.1175/1520-0477(2001)082<0659:IGAASF>2.3.CO;2

Huffman, G.J., Bolvin, D.T., Nelkin, E.J., 2017. Integrated Multi-satellitE Retrievals for GPM (IMERG) Technical Documentation.

Huffman, G.J., Bolvin, D.T., Nelkin, E.J., Wolff, D.B., Adler, R.F., Gu, G., Hong, Y., Bowman, K.P., Stocker, E.F., 2007. The TRMM Multisatellite Precipitation Analysis (TMPA): Quasi-global, multiyear, combined-sensor precipitation estimates at fine scales. J. Hydrometeorol. 8, 38–55. https://doi.org/10.1175/JHM560.1

Kidd, C., Becker, A., Huffman, G.J., Muller, C.L., Joe, P., Skofronick-Jackson, G., Kirschbaum, D.B., 2017. So, how much of the Earth’s surface is covered by rain gauges? Bull. Am. Meteorol. Soc. 98, 69–78. https://doi.org/10.1175/BAMS-D-14-00283.1

Kidd, C., Levizzani, V., 2011. Status of satellite precipitation retrievals. Hydrol. Earth Syst. Sci. 15, 1109–1116. https://doi.org/10.5194/hess-15-1109-2011

Kousky, V.E., 1988. Pentad outgoing longwave radiation climatology for the South American sector. Rev. Bras. Meteorol. 3, 217–231.

Laverde-Barajas, M., Corzo Perez, G.A., Dalfré Filho, J.G., Solomatine, D.P., 2018. Assessing the performance of near real-time rainfall products to represent spatiotemporal characteristics of extreme events: case study of a subtropical catchment in south-eastern Brazil. Int. J. Remote Sens. 39, 7568–7586. https://doi.org/10.1080/01431161.2018.1475773

Lelis, L., Bosquilia, R., Duarte, S., 2018. Assessment of precipitation data generated by GPM and TRMM satellites. Rev. Bras. Meteorol. 33, 153–163. https://doi.org/http://dx.doi.org/10.1590/0102-7786331004 rbmet.org.br Artigo

Levizzani, V., Kidd, C., Aonashi, K., Bennartz, R., Ferraro, R.R., Huffman, G.J., Roca, R., Turk, F.J., Wang, N.Y., 2018. The activities of the International Precipitation Working Group. Q. J. R. Meteorol. Soc. https://doi.org/10.1002/qj.3214

Lewis, E., Fowler, H., Alexander, L., Dunn, R., McClean, F., Barbero, R., Guerreiro, S., Li, X.-F., Blenkinsop, S., 2019. GSDR: A global sub-daily rainfall dataset. J. Clim. 32, 4715–4729. https://doi.org/10.1175/JCLI-D-18-0143.1

Lewis, E., Quinn, N., Blenkinsop, S., Fowler, H.J., Freer, J., Tanguy, M., Hitt, O., Coxon, G., Bates, P., Woods, R., 2018. A rule based quality control method for hourly rainfall data and a 1 km resolution gridded hourly rainfall dataset for Great Britain: CEH-GEAR1hr. J. Hydrol. 564, 930–943. https://doi.org/10.1016/j.jhydrol.2018.07.034

Li, R., Wang, K., Qi, D., 2018. Validating the Integrated Multisatellite Retrievals for Global Precipitation Measurement in terms of diurnal variability with hourly gauge observations collected at 50,000 stations in China. J. Geophys. Res. Atmos. 123, 10,423-10,442. https://doi.org/10.1029/2018JD028991

Lumbroso, D.M., Boyce, S., Bast, H., Walmsley, N., 2011. The challenges of developing rainfall intensity-duration-frequency curves and national flood hazard maps for the Caribbean. J. Flood Risk Manag. 4, 42–52. https://doi.org/10.1111/j.1753-318X.2010.01088.x

Mayor, Y.G., Tereshchenko, I., Fonseca-Hernández, M., Pantoja, D.A., Montes, J.M., 2017. Evaluation of error in IMERG precipitation estimates under different topographic conditions and temporal scales over Mexico. Remote Sens. 9, 1–18. https://doi.org/10.3390/rs9050503

Medeiros, P.H.A., Araújo, J.C., 2014. Temporal variability of rainfall in a semiarid environment in Brazil and its effect on sediment transport processes. J. Soils Sediments 14, 1216–1223. https://doi.org/10.1007/s11368-013-0809-9

Medina-Cobo, M.T., García-Marín, A.P., Estévez, J., Ayuso-Muñoz, J.L., 2016. The identification of an appropriate Minimum Inter-event Time (MIT) based on multifractal characterization of rainfall data series. Hydrol. Process. 30, 3507–3517. https://doi.org/10.1002/hyp.10875

Meier, C.I., Sebastián Moraga, J., Pranzini, G., Molnar, P., 2016. Describing the interannual variability of precipitation with the derived distribution approach: Effects of record length and resolution. Hydrol. Earth Syst. Sci. 20, 4177–4190. https://doi.org/10.5194/hess-20-4177-2016

Melo, D. de C.D., Xavier, A.C., Bianchi, T., Oliveira, P.T.S., Scanlon, B.R., Lucas, M.C., Wendland, E., 2015. Performance evaluation of rainfall estimates by TRMM multi-satellite precipitation analysis 3B42V6 and V7 over Brazil. J. Geophys. Res. 120, 9426–9436. https://doi.org/10.1002/2015JD023797

Molina-Sanchis, I., Lázaro, R., Arnau-Rosalén, E., Calvo-Cases, A., 2016. Rainfall timing and runoff : The influence of the criterion for rain event separation separation. J. Hydrol. Hydromechanics 64, 226–236. https://doi.org/10.1515/johh-2016-0024

Naumann, G., Barbosa, P., Carrao, H., Singleton, A., Vogt, J., 2012. Monitoring drought conditions and their uncertainties in Africa using TRMM data. J. Appl. Meteorol. Climatol. 51, 1867–1874. https://doi.org/10.1175/JAMC-D-12-0113.1

Nikolopoulos, E.I., Anagnostou, E.N., Borga, M., 2013. Using high-resolution satellite rainfall products to simulate a major flash flood event in northern Italy. J. Hydrometeorol. 14, 171–185. https://doi.org/10.1175/JHM-D-12-09.1

O, S., Foelsche, U., Kirchengast, G., Fuchsberger, J., Tan, J., Petersen, W.A., 2017. Evaluation of GPM IMERG Early, Late, and Final rainfall estimates using WegenerNet gauge data in southeastern Austria. Hydrol. Earth Syst. Sci. 21, 6559–6572. https://doi.org/10.5194/hess-21-6559-2017

O, S., Kirstetter, P.E., 2018. Evaluation of diurnal variation of GPM IMERG-derived summer precipitation over the contiguous US using MRMS data. Q. J. R. Meteorol. Soc. https://doi.org/10.1002/qj.3218

Ogallo, L.J., 1989. The spatial and temporal patterns of the East African seasonal rainfall derived from principal component analysis. Int. J. Climatol. 9, 145–167. https://doi.org/10.1002/joc.3370090204

Oliveira, R., Maggioni, V., Vila, D., Morales, C., 2016. Characteristics and diurnal cycle of GPM rainfall estimates over the Central Amazon region. Remote Sens. 8. https://doi.org/10.3390/rs8070544

Oliveira, R., Maggioni, V., Vila, D., Porcacchia, L., 2018. Using satellite error modeling to improve GPM-Level 3 rainfall estimates over the central Amazon region. Remote Sens. 10. https://doi.org/10.3390/rs10020336

Pombo, S., de Oliveira, R.P., 2015. Evaluation of extreme precipitation estimates from TRMM in Angola. J. Hydrol. 523, 663–679. https://doi.org/10.1016/j.jhydrol.2015.02.014

Prakash, S., Mitra, A.K., Aghakouchak, A., Liu, Z., Norouzi, H., Pai, D.S., 2018. A preliminary assessment of GPM-based multi-satellite precipitation estimates over a monsoon dominated region. J. Hydrol. 556, 865–876. https://doi.org/10.1016/j.jhydrol.2016.01.029

Reboita, M.S., Gan, M.A., Rocha, R.P., Ambrizzi, T., 2010. Precipitation regimes in South America: a bibliography review. Rev. Bras. Meteorol. 25, 185–204.

Renard, K.G., Foster, G.R., Weesies, G.A., Porter, J.P., 1997. Predicting soil erosion by water: a guide to conservation planning with the Revised Universal Soil Loss Equation (RUSLE). U.S. Department of Agriculture, Agriculture Handbook No. 703, Washington D.C. https://doi.org/10.1201/9780203739358-5

Rozante, J.R. and, Vila, D.A. and, Chiquetto, Júlio Barboza and Fernandes, A. de A. and, Alvim, D.S., 2018. Evaluation of TRMM/GPM Blended Daily Products over Brazil. Remote Sens. 15, 814–815. https://doi.org/https://doi.org/10.3390/rs10060882

Salles, L., Satgé, F., Roig, H., Almeida, T., Olivetti, D., Ferreira, W., 2019. Seasonal effect on spatial and temporal consistency of the new GPM-based IMERG-v5 and GSMaP-v7 satellite precipitation estimates in Brazil's Central Plateau Region. Water 11, 668. https://doi.org/10.3390/w11040668

Satgé, F., Ruelland, D., Bonnet, M.P., Molina, J., Pillco, R., 2019. Consistency of satellite-based precipitation products in space and over time compared with gauge observations and snow- hydrological modelling in the Lake Titicaca region. Hydrol. Earth Syst. Sci. 23, 595–619. https://doi.org/10.5194/hess-23-595-2019

Satgé, F., Xavier, A., Zolá, R.P., Hussain, Y., Timouk, F., Garnier, J., Bonnet, M.P., 2017. Comparative assessments of the latest GPM mission's spatially enhanced satellite rainfall products over the main bolivian watersheds. Remote Sens. 9, 1–16. https://doi.org/10.3390/rs9040369

Schneider, U., Becker, A., Finger, P., Meyer-Christoffer, A., Ziese, M., Rudolf, B., 2014. GPCC's new land surface precipitation climatology based on quality-controlled in situ data and its role in quantifying the global water cycle. Theor. Appl. Climatol. 115, 15–40. https://doi.org/10.1007/s00704-013-0860-x

Singh, C.V., 2006. Pattern characteristics of Indian monsoon rainfall using principal component analysis (PCA). Atmos. Res. 79, 317–326. https://doi.org/10.1016/j.atmosres.2005.05.006

Skofronick-Jackson, G., Kirschbaum, D., Petersen, W., Huffman, G., Kidd, C., Stocker, E., Kakar, R., 2018. The Global Precipitation Measurement (GPM) mission's scientific achievements and societal contributions: reviewing four years of advanced rain and snow observations. Q. J. R. Meteorol. Soc. https://doi.org/10.1002/qj.3313

Skofronick-Jackson, G., Petersen, W.A., Berg, W., Kidd, C., Stocker, E.F., Kirschbaum, D.B., Kakar, R., Braun, S.A., Huffman, G.J., Iguchi, T., Kirstetter, P.E., Kummerow, C., Meneghini, R., Oki, R., Olson, W.S., Takayabu, Y.N., Furukawa, K., Wilheit, T., 2017. The global precipitation measurement (GPM) mission for science and Society. Bull. Am. Meteorol. Soc. 98, 1679–1695. https://doi.org/10.1175/BAMS-D-15-00306.1

Skofronick- Jackson, G., Kirschbaum, D., Petersen, W., Huffman, G., Kidd, C., Stocker, E., Kakar, R., 2018. The Global Precipitation Measurement (GPM) mission's scientific achievements and societal contributions: reviewing four years of advanced rain and snow observations. Q. J. R. Meteorol. Soc. 144, 27–48. https://doi.org/10.1002/qj.3313

Tan, J., Huffman, G.J., Bolvin, D.T., Nelkin, E.J., 2019. IMERG V06: Changes to the Morphing Algorithm. J. Atmos. Ocean. Technol. 36, 2471–2482. https://doi.org/10.1175/JTECH-D-19-0114.1

Tan, J., Petersen, W.A., Kirstetter, P.-E., Tian, Y., 2017. Performance of IMERG as a Function of Spatiotemporal Scale. J. Hydrometeorol. 18, 307–319. https://doi.org/10.1175/JHM-D-16-0174.1

Tan, M., Duan, Z., 2017. Assessment of GPM and TRMM Precipitation Products over Singapore. Remote Sens. 9, 720. https://doi.org/10.3390/rs9070720

Tang, G., Behrangi, A., Long, D., Li, C., Hong, Y., 2018. Accounting for spatiotemporal errors of gauges: A critical step to evaluate gridded precipitation products. J. Hydrol. 559, 294–306. https://doi.org/10.1016/j.jhydrol.2018.02.057

Tang, G., Ma, Y., Long, D., Zhong, L., Hong, Y., 2016a. Evaluation of GPM Day-1 IMERG and TMPA Version-7 legacy products over Mainland China at multiple spatiotemporal scales. J. Hydrol. 533, 152–167. https://doi.org/10.1016/j.jhydrol.2015.12.008

Tang, G., Zeng, Z., Long, D., Guo, X., Yong, B., Zhang, W., Hong, Y., 2016b. Statistical and Hydrological Comparisons between TRMM and GPM Level-3 Products over a Midlatitude Basin: Is Day-1 IMERG a Good Successor for TMPA 3B42V7? J. Hydrometeorol. 17, 121–137. https://doi.org/10.1175/JHM-D-15-0059.1

Tian, F., Hou, S., Yang, L., Hu, H., Hou, A., 2018. How does the evaluation of the gpm imerg rainfall product depend on gauge density and rainfall intensity? J. Hydrometeorol. 19, 339–349. https://doi.org/10.1175/JHM-D-17-0161.1

Velasco, I., Fritsch, J.M., 1987. Mesoscale convective complexes in the Americas. J. Geophys. Res. 92, 9591. https://doi.org/10.1029/JD092iD08p09591

Wang, C., Tang, G., Han, Z., Guo, X., Hong, Y., 2018. Global intercomparison and regional evaluation of

GPM IMERG Version-03, Version-04 and its latest Version-05 precipitation products: Similarity, difference and improvements. J. Hydrol. 564, 342–356. https://doi.org/10.1016/j.jhydrol.2018.06.064

Westra, S., Fowler, H.J., Evans, J.P., Alexander, L. V., Berg, P., Johnson, F., Kendon, E.J., Lenderink, G., Roberts, N.M., 2014. Future changes to the intensity and frequency of short-duration extreme rainfall. Rev. Geophys. 52, 522–555. https://doi.org/10.1002/2014RG000464

Wischmeier, W.H., Smith, D.D., 1978. Predicting rainfall erosion losses - a guide to conservation planning. U.S. Department of Agriculture, Agriculture Handbook No. 537, Washington D.C.

WMO, 1994. Guide to hydrological practices: Data acquisition and processing, analysis, forecasting and other applications.

Yang, X., Yong, B., Hong, Y., Chen, S., Zhang, X., 2016. Error analysis of multi-satellite precipitation estimates with an independent raingauge observation network over a medium-sized humid basin. Hydrol. Sci. J. 1–18. https://doi.org/10.1080/02626667.2015.1040020

Yuan, F., Zhang, L., Soe, K., Ren, L., Zhao, C., Zhu, Y., Jiang, S., Liu, Y., 2019. Applications of TRMM- and GPM-Era Multiple-Satellite Precipitation Products for flood simulations at sub-daily scales in a sparsely gauged watershed in Myanmar. Remote Sens. 11, 140. https://doi.org/10.3390/rs11020140

Figure 1

Click here to download high resolution image

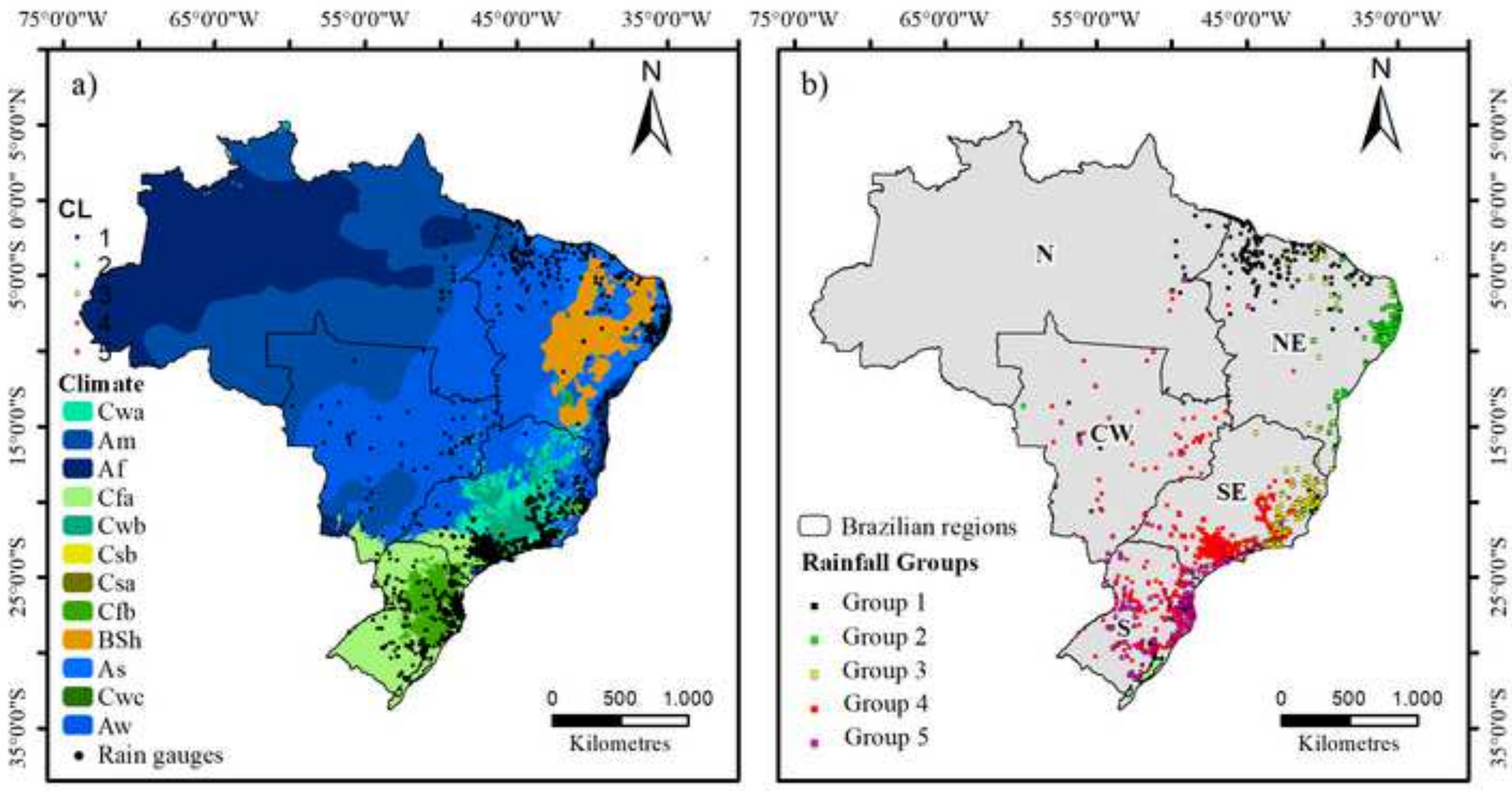

Figure_2
Click here to download high resolution image

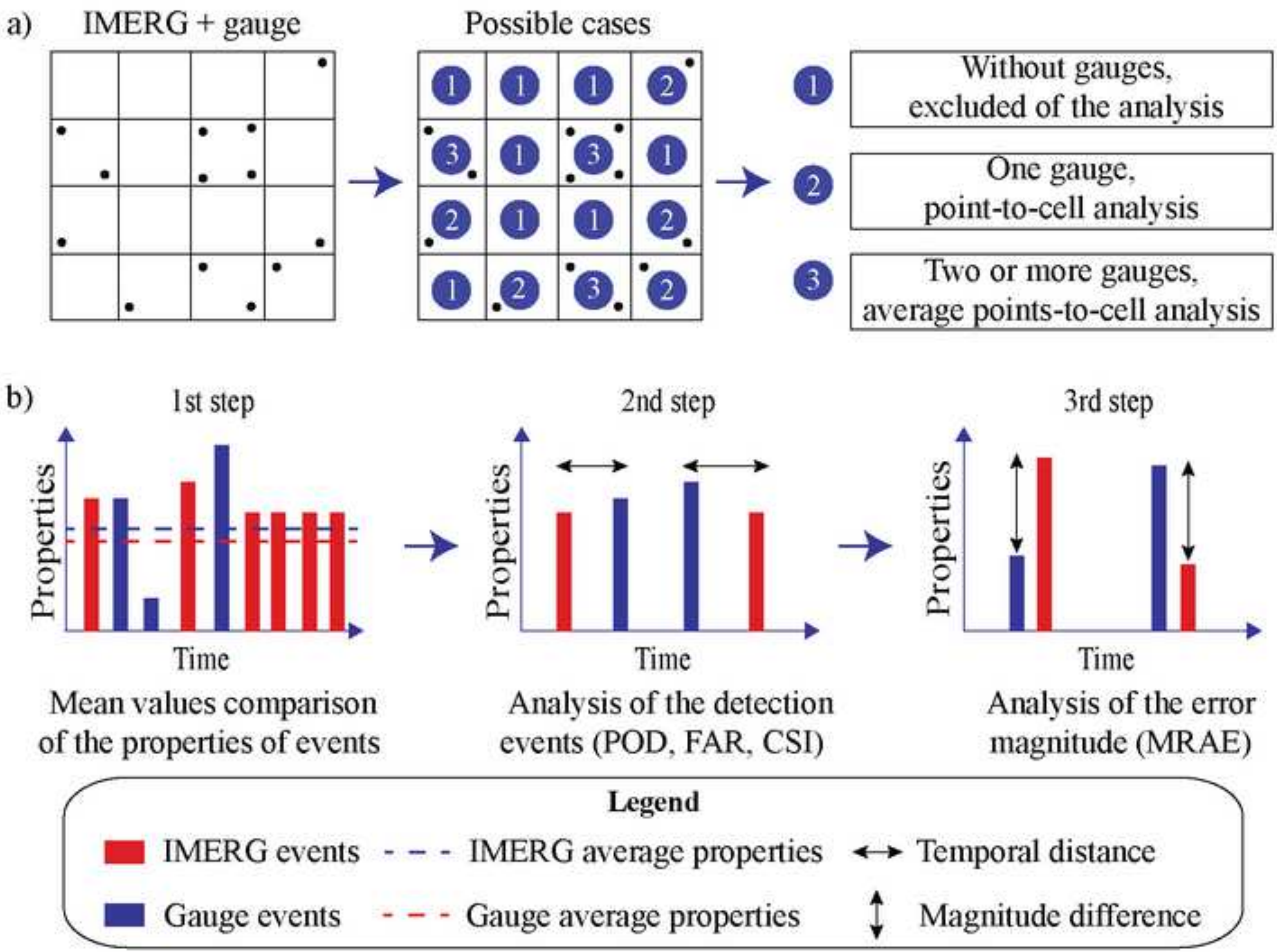

Figure 3

Click here to download high resolution image

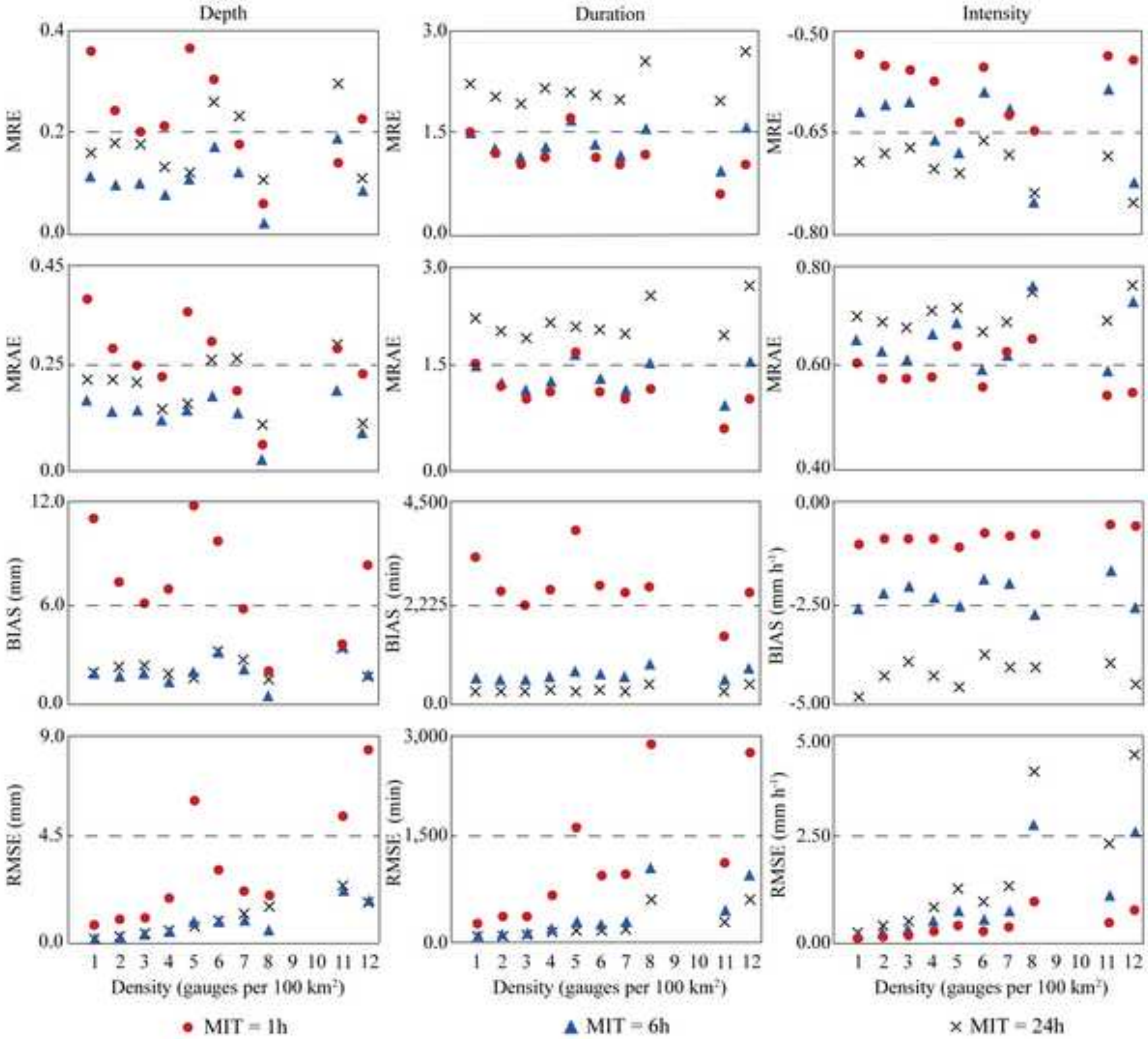

Figure_4
Click here to download high resolution image

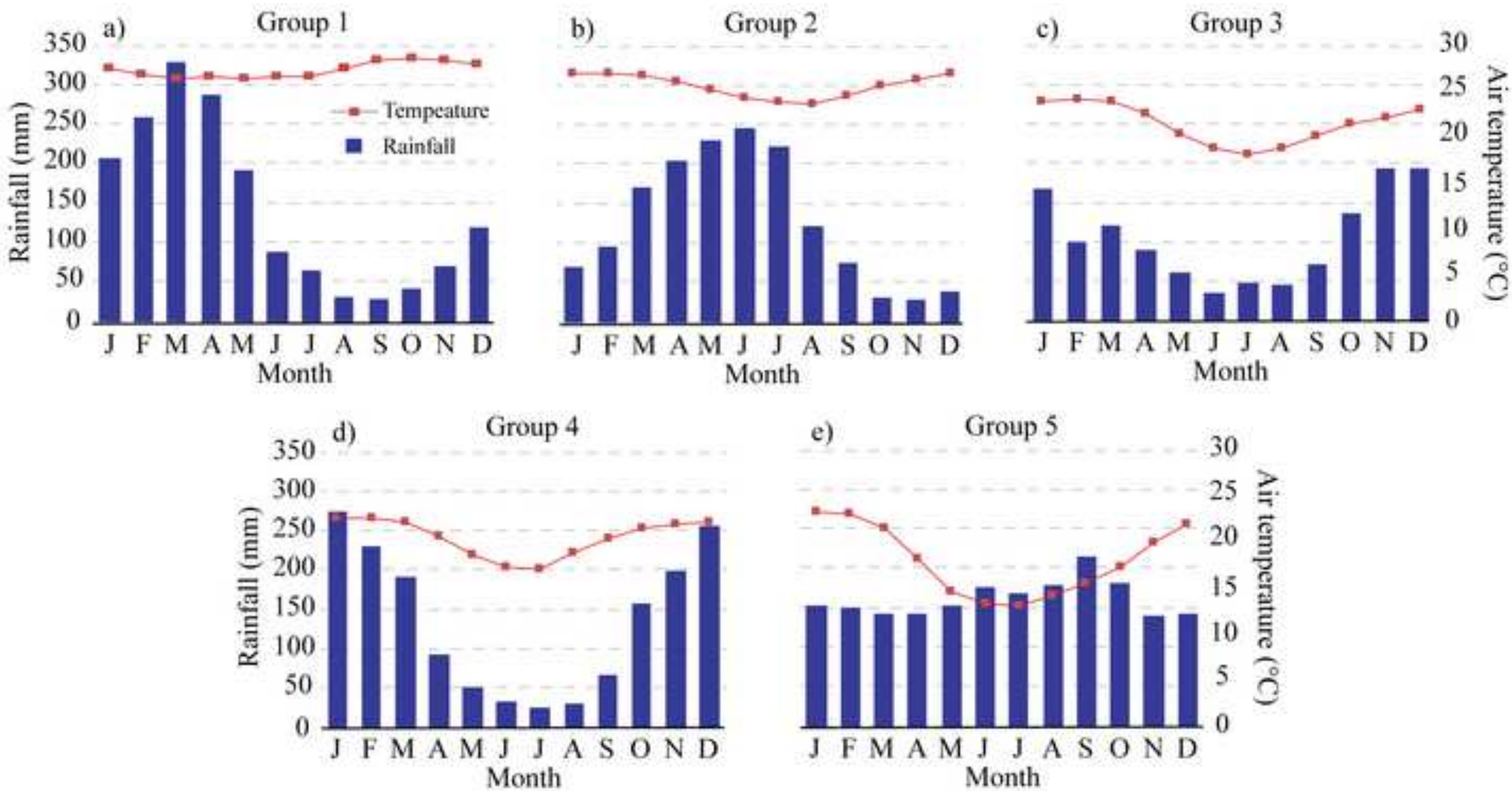

Figure_5
Click here to download high resolution image

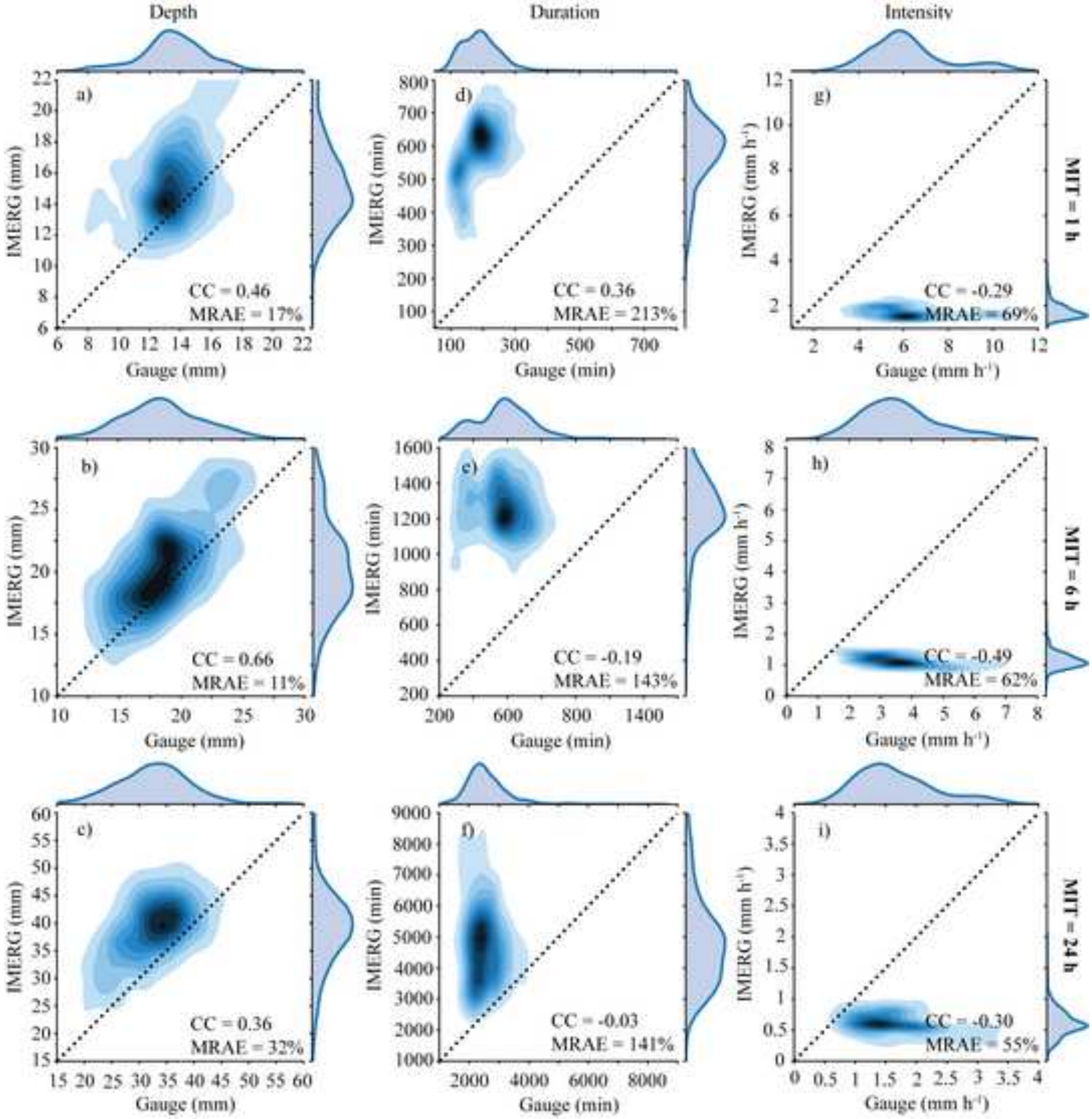

Figure_6

Click here to download high resolution image

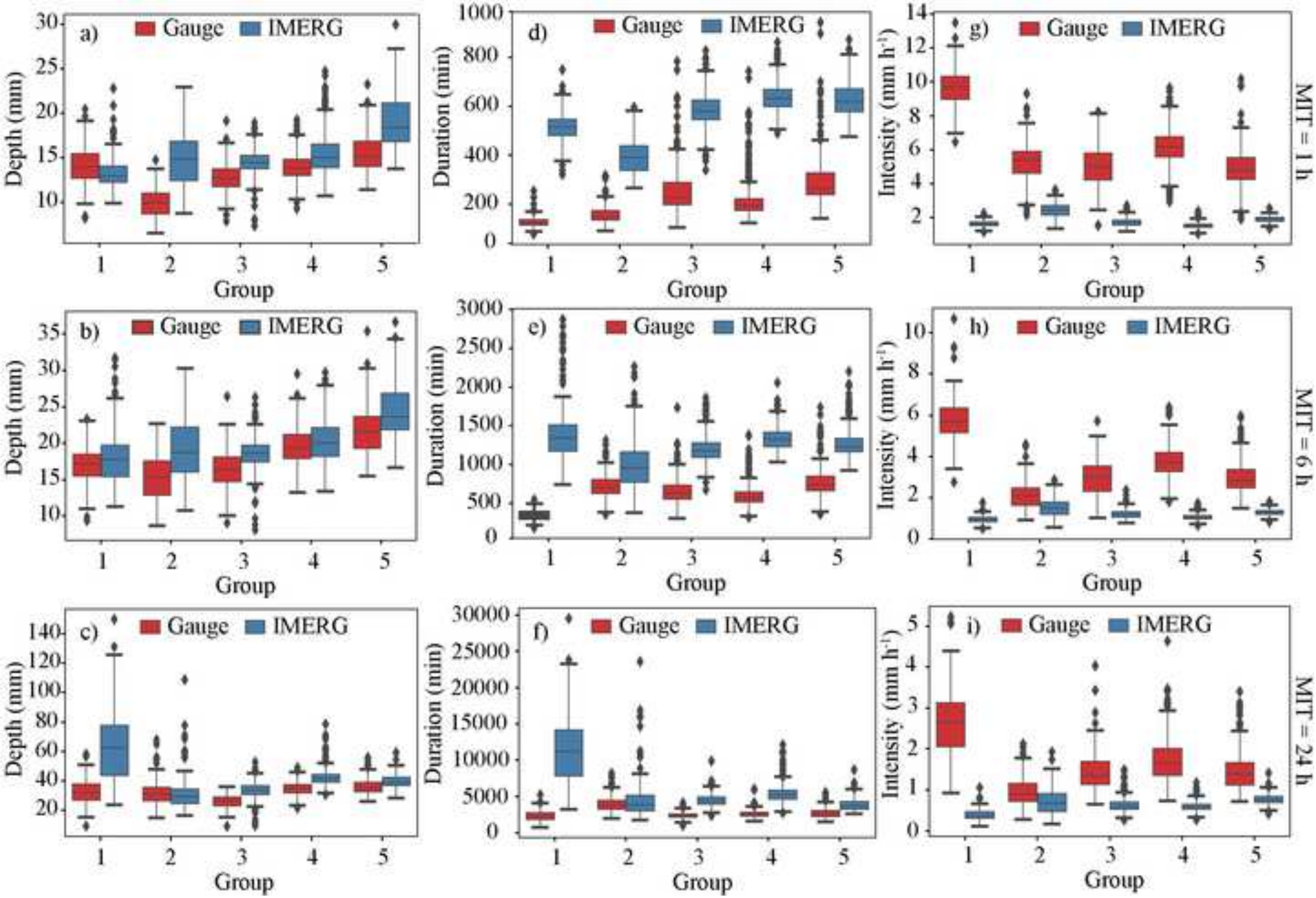

Figure_7

Click here to download high resolution image

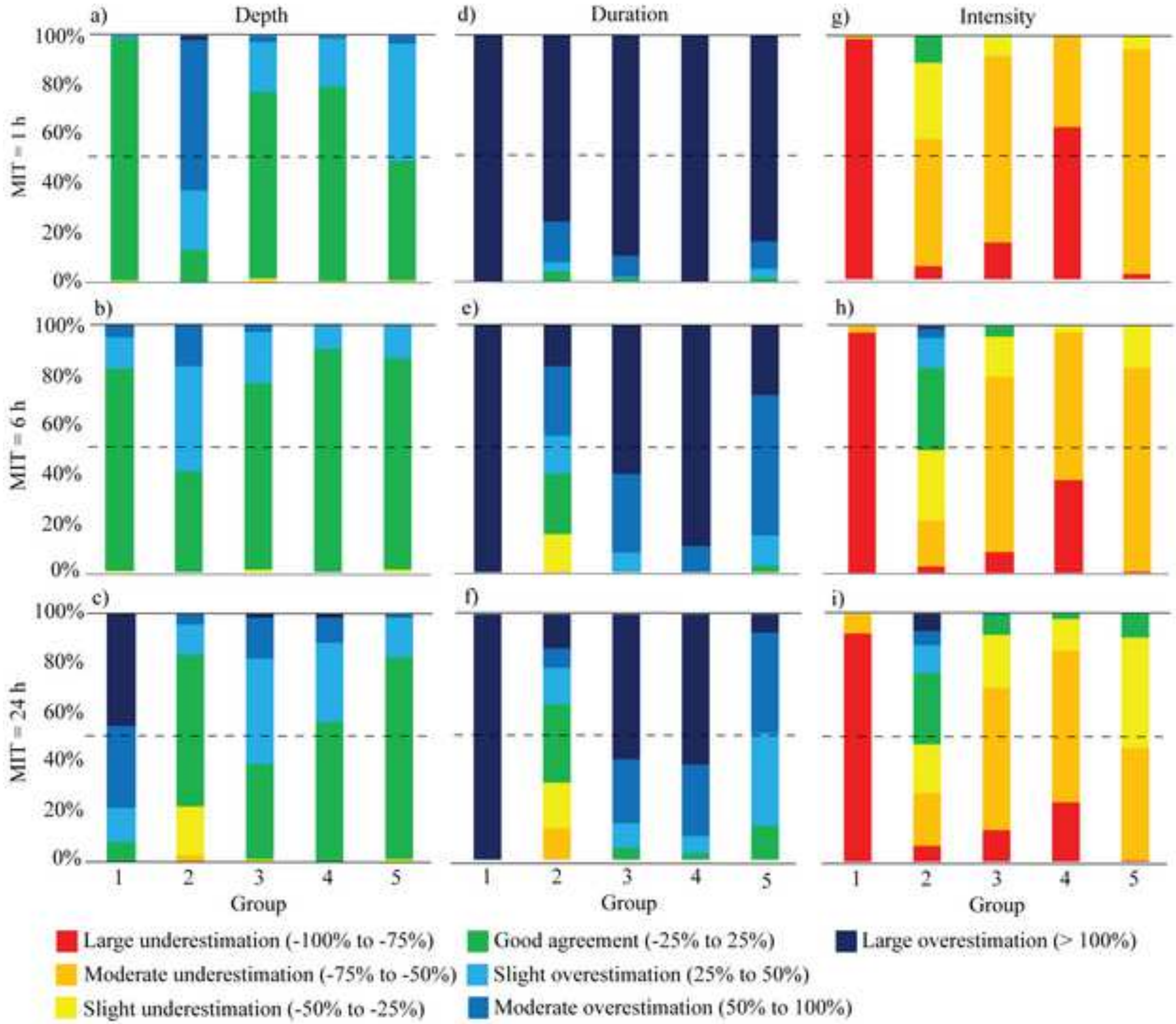

Figure_8
Click here to download high resolution image

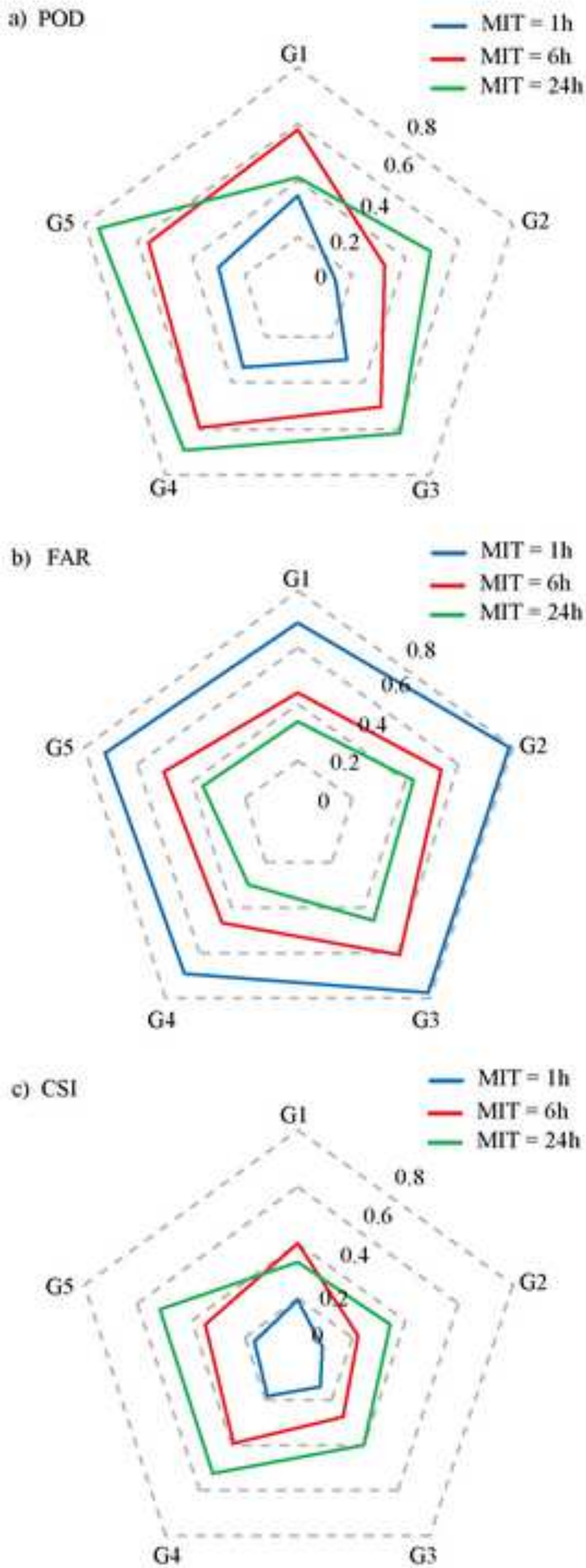

Figure_9
Click here to download high resolution image

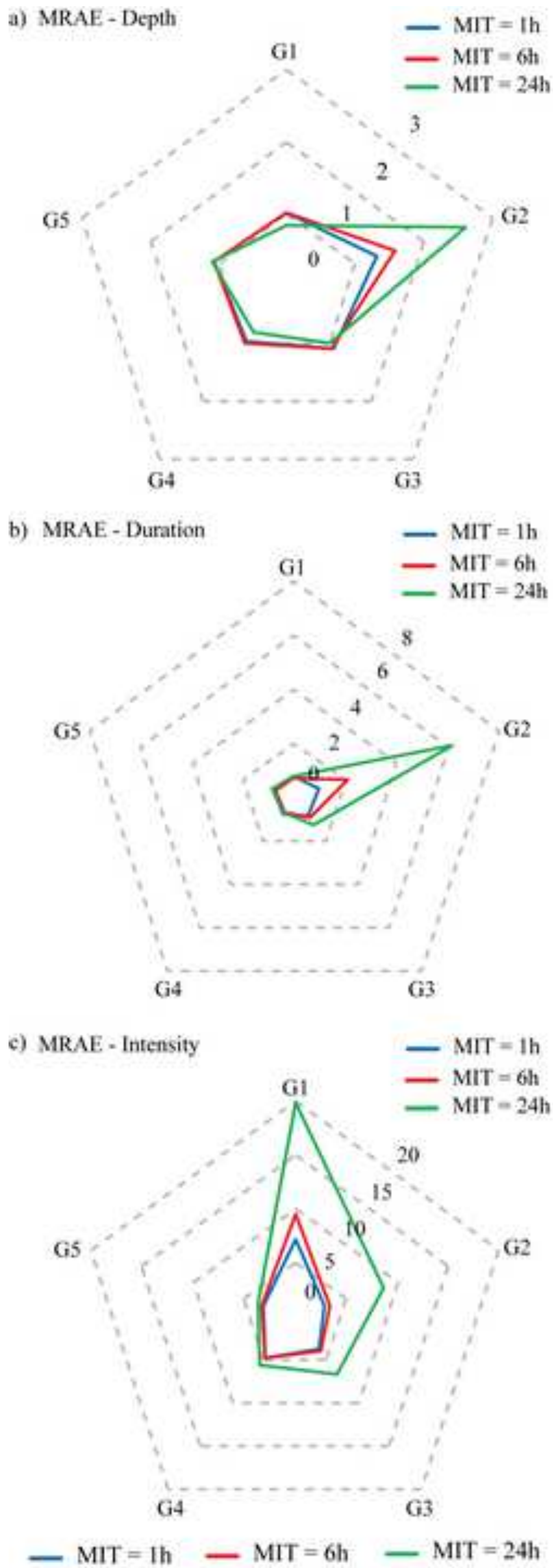

Table 1

Table 1 Summary of relevant characteristics of each homogeneous rainfall group, including the rainfall regimes defined by Reboita et al. (2010).

Group	Number of Pixels	Annual rainfall (mm)	Climate*	Atmospheric Systems
1	163	1,400 – 2,000	Tropical monsoon (Am) and Tropical with dry winter (Aw)	Intertropical Convergence Zone (ITCZ) and Mesoscale Convective Complex (MCC)
2	108	1,200 – 1,800	Tropical with dry summer (As)	Instability Lines (IL) and Southeast Trade Winds (SETW)
3	209	1,000 – 1,300	Tropical with dry summer (As)	South Atlantic Subtropical Anticyclone (SASA) and South Atlantic Convergence Zone (SACZ)
4	317	1,300 – 1,900	Humid subtropical with dry winter (Cw)	South Atlantic Subtropical Anticyclone (SASA) and South Atlantic Convergence Zone (SACZ)
5	268	1,600 – 2,200	Humid subtropical with hot summer (Cfa)	Prefrontal Squall Line (PSL) and Cold Fronts (CF)

* According to Köppen's classification proposed by Alvares et al. (2013).

Table 2
Click here to download Table: Table 2_Paper_Freitas_et_al_HIDROL33715.docx

Table 2. Rain gauge densities per grid cells used in this study.

Gauges per grid cell	Number of grid cells	Percentage of grid cells
1	775	69.0
2	169	15.9
3	82	7.7
4	30	2.8
5	16	1.5
6	18	1.7
7	10	1.5
8	1	0.3
9	0	0
10	0	0
11	3	0.3
12	1	0.1
Total	1065	100.0

Table 3

Click here to download Table: Table 3_Paper_Freitas_et_al_HIDROL33715.docx

Table 3. Summary of evaluation metrics for the IMERG-F product, considering the mean values of rainfall properties for each homogeneous group.

Group		Depth (mm)			Duration (min)			Intensity (mm/h)		
		MIT=1h	**MIT=6h**	**MIT=24h**	**MIT=1h**	**MIT=6h**	**MIT=24h**	**MIT=1h**	**MIT=6h**	**MIT=24h**
1	CC	0.57	0.52	0.67	0.29	0.64	0.57	-0.12	0.34	0.30
	MRAE (%)	11.0	15.8	98.7	322.2	321.0	415.5	82.7	83.5	84.7
2	CC	0.59	0.69	0.30	-0.36	-0.54	-0.42	-0.37	-0.61	-0.22
	MRAE (%)	55.2	30.7	23.2	158.5	64.4	57.9	48.7	36.9	49.9
3	CC	0.14	0.42	0.55	0.12	0.21	-0.06	-0.11	-0.28	-0.14
	MRAE (%)	17.2	17.3	34.1	177.4	113.7	116.0	66.9	59.7	56.2
4	CC	0.14	0.36	0.22	0.31	0.08	0.01	-0.14	-0.19	-0.16
	MRAE (%)	15.0	11.6	28.5	253.1	153.8	128.0	75.4	72.3	63.8
5	CC	0.38	0.42	0.30	-0.02	0.17	0.47	0.27	0.31	0.43
	MRAE (%)	25.0	14.4	14.9	150.2	81.9	54.3	62.9	57.7	46.2